2008

A Validation of the FSU/COAPS Climate Model

Mary Beth Engelman

FLORIDA STATE UNIVERSITY

COLLEGE OF ARTS AND SCIENCES

A VALIDATION OF THE FSU/COAPS CLIMATE MODEL

By

MARY BETH ENGELMAN

A Thesis submitted to the
Department of Meteorology
in partial fulfillment of the
requirements for the degree of
Masters of Science

Degree Awarded:
Fall Semester, 2008

The members of the Committee approve the thesis of Mary Beth Engelman defended on August 13, 2008.

_____
James J. O'Brien
Professor Co-Directing Thesis

_____
Jon E. Ahlquist
Professor Co-Directing Thesis

_____
Paul H. Ruscher
Committee Member

_____
Timothy E. LaRow
Committee Member

The Office of Graduate Studies has verified and approved the above named committee members.

I dedicate this paper to my parents for their unconditional love and support from my first day of kindergarten through my last day of graduate school.

ACKNOWLEDGEMENTS

Several friends, family, and faculty deserve many thanks for their assistance to the completion of this paper. First of all, I would like to thank Dr. James O'Brien for offering me a research position at COAPS and providing me with the needed resources to complete this study. In addition, I would like to thank Dr. Jon Ahlquist for signing on as a co-adviser as well as Dr. Paul Rusher who was also willing to serve on my committee. I am especially grateful for Dr. Tim LaRow and the rest of the climate group at COAPS for offering excellent guidance and advice throughout the research and writing process. Thanks also to the entire COAPS staff for all the comments, suggestions, and support during student presentations and some of those particularly long work days. Of course, a huge thanks is deserved to those who offered consistent encouragement and support both at school and at home. This includes parents, family, friends, and even future in-laws. I especially appreciated all my out-of-town visitors. Finally, a special thanks goes to my fiancé and best friend, Glenn, for always being so understanding.

TABLE OF CONTENTS

LIST OF TABLES

LIST OF FIGURES

ABSTRACT

This study examines the predictability of the Florida State University/Center for Oceanic and Atmospheric Prediction Studies (FSU/COAPS) climate model, and is motivated by the model's potential use in crop modeling. The study also compares real-time ensemble runs (created using persisted SST anomalies) to hindcast ensemble runs (created using weekly updated SST) to asses the effect of SST anomalies on forecast error. Wintertime (DJF, 2 month lead time) surface temperature and precipitation forecasts over the southeastern United States (Georgia, Alabama, and Florida) are evaluated because of the documented links between tropical Pacific SST anomalies and climate in the southeastern United States during the winter season. The global spectral model (GSM) runs at a T63 resolution and then is dynamically downscaled to a 20 x 20 km grid over the southeastern United States using the FSU regional spectral model (RSM). Seasonal, monthly, and daily events from the October 2004 and 2005 model runs are assessed. Seasonal (DJF) plots of real-time forecasts indicate the model is capable of predicting wintertime maximum and minimum temperatures over the southeastern United States. The October 2004 and 2005 real-time model runs both produce temperature forecasts with anomaly errors below 3°C, correlations close to one, and standard deviations similar to observations. Real-time precipitation forecasts are inconsistent. Error in the percent of normal precipitation vary from greater than 100% in the 2004/2005 forecasts to less than 35% error in the 2005/2006 forecasts. Comparing hindcast runs to real-time runs reveals some skill is lost in precipitation forecasts when using a method of SST anomaly persistence if the SST anomalies in the equatorial Pacific change early in the forecast period, as they did for the October 2004 model runs. Further analysis involving monthly and daily model data as well as Brier scores (BS), relative operating characteristics (ROC), and equitable threat scores (ETS), are also examined to confirm these results.

CHAPTER 1
INTRODUCTION

Climate and seasonal prediction continues to make rapid advances in the atmospheric sciences. Seasonal predictions are possible in part due to the strong relationship that exists between the global atmosphere and the tropical oceans. Probably the best known relationship between the atmosphere and tropical ocean, in particular the tropical Pacific, is the El Nino – Southern Oscillation (ENSO). The ENSO cycle typically lasts three to seven years. During the warm phase of the cycle, anomalously warm tropical Pacific sea surface temperatures (SSTs) develop in the eastern tropical Pacific, a result of wind-forced equatorial Rossby and Kelvin waves (Wyrtki 1975; Hurlburt et al. 1976; etc.). Large-scale atmospheric response (notably changes to the Hadley and Walker circulations) to the anomalous tropical ocean forcing was first discussed by Bjerknes (1966). Since then, other such low frequency quasi-stationary large-scale anomalous atmospheric patterns have been discovered. These patterns are typically termed teleconnections. Teleconnections develop as part of internal atmosphere dynamics or in response to anomalous tropical SSTs and the resulting tropical atmospheric convection. The latter is particularly true for the Pacific/North American (PNA) mode and the Madden-Julian Oscillation (MJO). The ability of climate models to simulate the development and atmospheric response of these teleconnections offer the potential for seasonal climate predictability to several parts of the globe (see Bjerknes 1966; Ropelewski and Halpert 1987, 1989; Goddard et al. 2001; Wilks and Wilby 1999). Today's sophisticated climate models, which include coupled ocean-atmospheric models, effectively utilize some of these oscillations to simulate future climate (Goddard et al. 2001). Despite these advances in climate prediction, a forecast of climatology still remains difficult to beat. Outperforming climatology becomes especially challenging in areas with minimal ENSO signals and during neutral or even weak ENSO phases (Goddard et al. 2001). As the understanding of the climate and the number of models integrated for seasonal and longer term predictions increases, so does the need for model verification.

This study is an evaluation of real-time seasonal forecasts computed by the Florida State University/Center of Ocean-Atmosphere Prediction Studies (FSU/COAPS) regional climate model (Cocke and LaRow 2000). These sets of experiments are called "real-time". An additional set of experiments are conducted for the same time period using observed SSTs, referred to as "hindcasts". This study compares both real-time and hindcast runs during the boreal wintertime. Seasonal, monthly, and daily precipitation and surface land temperature forecasts over the southeastern United States are examined.

One motivation for this study stems from the benefits it offers to society. Agriculture plays a major role in the southeast's economy. The 2002 Census of Agriculture approximated the market value of agricultural products sold for Florida, Georgia, and Alabama combined to be over fourteen billion dollars (http://www.agcensus.usda.gov/). Unanticipated extreme weather events can significantly impact this number. For example, the 1997-1998 El Nino event caused an estimated 165 million dollars of agricultural losses in Florida alone (Florida Department of Agriculture, http://www.doacs.state.fl.us/). Currently, organizations such as the Southeast Climate Consortium and AgClimate combine their various climate forecasts and crop yields in an attempt to better prepare farmers of Florida, Georgia, and Alabama for the upcoming growing season. The output of the FSU/COAPS climate model is currently being examined for use in crop models in an effort to minimize losses and maximize profits for farmers in the southeastern United States.

Benefits to the science also motivate this study. Currently, the FSU/COAPS global model is not coupled to an ocean model for crop applications. In general, coupled ocean-atmosphere models cannot produce sea surface temperature anomaly (SSTA) forecasts that outperform a method of SSTA persistence at lead times less than three months; however, the use of a coupled-ocean atmosphere model to simulate climate seems inevitable with the undeniable links between SSTA and seasonal climate patterns (Goddard et al. 2001; Goddard and Mason 2002). Comparing real-time runs to hindcasts runs reveals limitations in the model associated with using persisted SSTA in climate forecasting. Also, model verification will lead to a better understanding of model errors and biases, which potentially leads to an improved climate model.

The primary objective of this study is to determine predictability of the FSU/COAPS real-time climate model forecasts of land surface temperature and precipitation over the southeastern United States. Previous studies that coupled the land-atmosphere model to an

ocean model concluded that the model is capable of reproducing larger-scale features associated with ENSO as well as teleconnection responses (Cocke and LaRow 2000; Cocke et al. 2007). These studies also showed that the regional and global model have similar results, which were both in reasonable agreement with observations from the winter season (Cocke and LaRow 2000; Cocke et al. 2007). More specifically, previous studies analyzing the model's ability to forecast temperature and precipitation determined that the regional model tends to over predict small rainfall events, but accurately produce larger rainfall events (Cocke et al. 2007). It should be noted that the regional model was not simply a spatial interpolation of the global model solution. A study that used prescribed SST's (hindcast runs) compared statistical and dynamical downscaling of the global model confirmed that the dynamical model successfully forecasts seasonal variations, anomalies, and changes in extreme daily events for maximum temperature (Lim et al. 2007). Also, early studies showed that the model had a wet bias and cold surface temperature bias, which were both reduced with the inclusion of the NCAR Community Land Model2 (Shin et al. 2005).

A secondary objective of this study is to examine how forecasts made from persisted observed SSTA compare to hindcasts made from weekly updated observed SSTs. Despite being an upper bound on skill, the analysis of the hindcasts runs measures the model's performance assuming a perfect SST forecast. Also, comparing real-time runs to hindcasts runs approximates how much skill can potentially be lost from using persisted SSTA versus a coupled ocean-atmosphere model, again, assuming the coupled model is perfect in simulating the SSTs. Goddard and Mason (2002) analyzed the sensitivity of seasonal precipitation forecasts to persisted SST anomalies and concluded that using persisted SSTA retains much of the precipitation skill that comes from using prescribed SST. The exception to this was when there were large fluctuations in the SSTA over the tropical oceans, which was expected because of the well known links between tropical SSTAs and climate (Bjerknes 1996; Goddard and Mason 2002). The links between climate in the southeastern United States and tropical Pacific SSTs are well documented. During El Nino events, the southeast conclusively experiences above normal wintertime precipitation and to a lesser extent, an El Nino event tends to lead to below normal wintertime temperatures in the southeast (Ropelewski and Halpert 1986; Montroy 1996; Gershunov and Barnett 1997; Smith et al. 1999). Ropelewski and Halpert (1986) also state that the ENSO response time varied for temperature and precipitation, suggesting that the physical

mechanisms driving these responses are different. Anomalies in the temperature pattern have a longer response time (December of the ENSO year through the following March) and are believed to be a result of the PNA circulation pattern driven by ENSO, where as the shorter response time of the precipitation anomalies (October of the ENSO year through the following March) suggest that they are due more to a direct link to ENSO rather than a teleconnection response.

In this study, forecasts from October 2004 and 2005 are examined. Before evaluating the model output, the real-time run's shortcomings against hindcasts runs can be anticipated by examining SSTA error growth in the tropical Pacific caused from using prescribed SSTA in the real-time runs (Figure 1.1). The error growth is defined as the forecasted SSTA minus the observed SSTA at each week of the forecast period. The SST data originates from the National Center for Environmental Prediction Studies (NCEP's) Optimum Interpolation version two (OI.v2) dataset. The dataset is a combination of in situ SSTs, satellite SSTs, and SSTs simulated by sea-ice cover. More details of the reanalysis, including Reynold's method of bias correction for the satellite data is available at (www.emc.ncep.noaa.gov/research/mb/ st_analysis/). In 2004, a large area (roughly 5-30˚N latitude, 110-150˚W longitude) of positive SSTA errors develops by week three of the forecast period and continues to grow through week eight of the forecast period, resulting in SSTA errors greater than 2˚C for a large portion of the tropical Pacific (Figure 1.1a). In 2005, positive errors develop in the tropical Pacific, but they are not as strong and do not nearly cover the same amount of area as they did in 2004 (Figure 1.1b). Based on previous studies of connections between tropical Pacific SSTA and climate in the southeastern United States, the real-time and hindcast runs should be more similar in 2005 than they are in 2004, with larger errors in the real-time runs in 2004.

Considering these previous studies and the examined SSTA error growth, when evaluating the FSU/COAPS regional climate model over the southeastern United States, the seasonal and monthly forecasts should show reasonable skill if the SSTAs in the tropical Pacific stay relatively constant, as they did during the first ten weeks of the October 2005 forecasts. Also, unless bias corrected, model data will show a wet bias in precipitation, particularly for small rainfall events, and a 2-4˚C cold bias in maximum surface temperature based on the study by Shin et al. (2005). When comparing the real-time runs to hindcast runs, the hindcasts runs should generally show more skill at lead times greater than three months; however, the two

forecasts should be comparable when equatorial Pacific SSTA remain relatively constant throughout the duration of forecast (Goddard and Mason 2002). A loss of skill in the real-time runs should occur when equatorial Pacific SSTA change signs, and if the SSTA do make a sizable transition (as they did by week 3 of the October 2004 forecast period), the largest loss of skill will occur where there are strong teleconnection signals, such as over the southeastern United States. Also, since neither of the years being evaluated were strong ENSO events, the model forecasts are expected to show similar or even less skill when compared to a forecast of climatology.

The next chapter briefly goes over the data used in this study as well as some details of the FSU/COAPS climate model. Chapter three and four display and discuss the results from temperature and precipitation model output, including the bias correction of data and how well the model forecasted seasonal and monthly anomalies as well as daily events. Finally, chapter five summarizes the study, states noteworthy conclusions, and discusses future work that could stem from these conclusions.

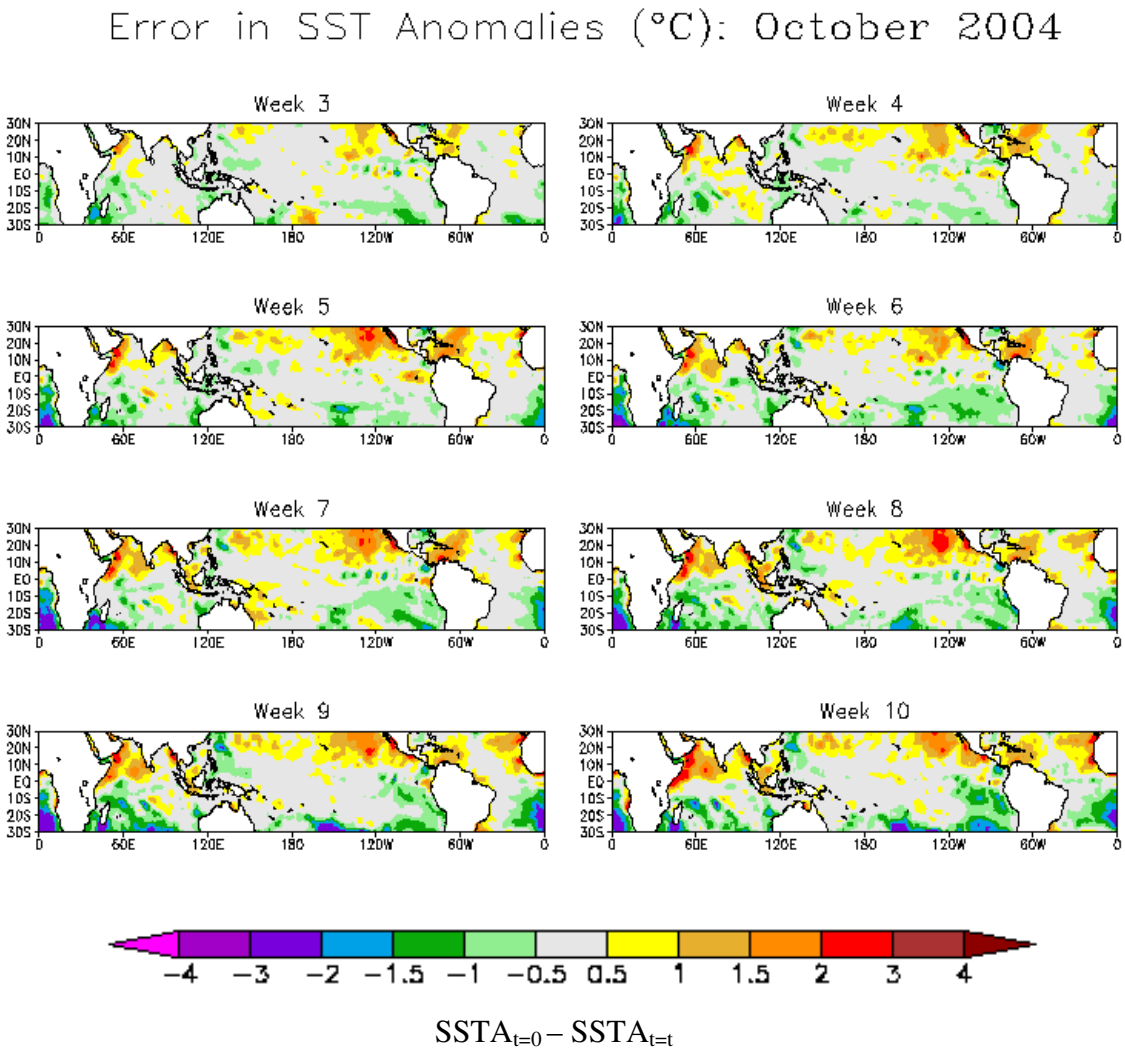

(a)

Figure 1.1. SSTA error growth (forecasted SSTA-observed SSTA) in the tropical Pacific (from weeks three through ten of the forecast period) resulting from using a prescribed SSTA in the October 2004 (a) and 2005 (b) real-time runs.

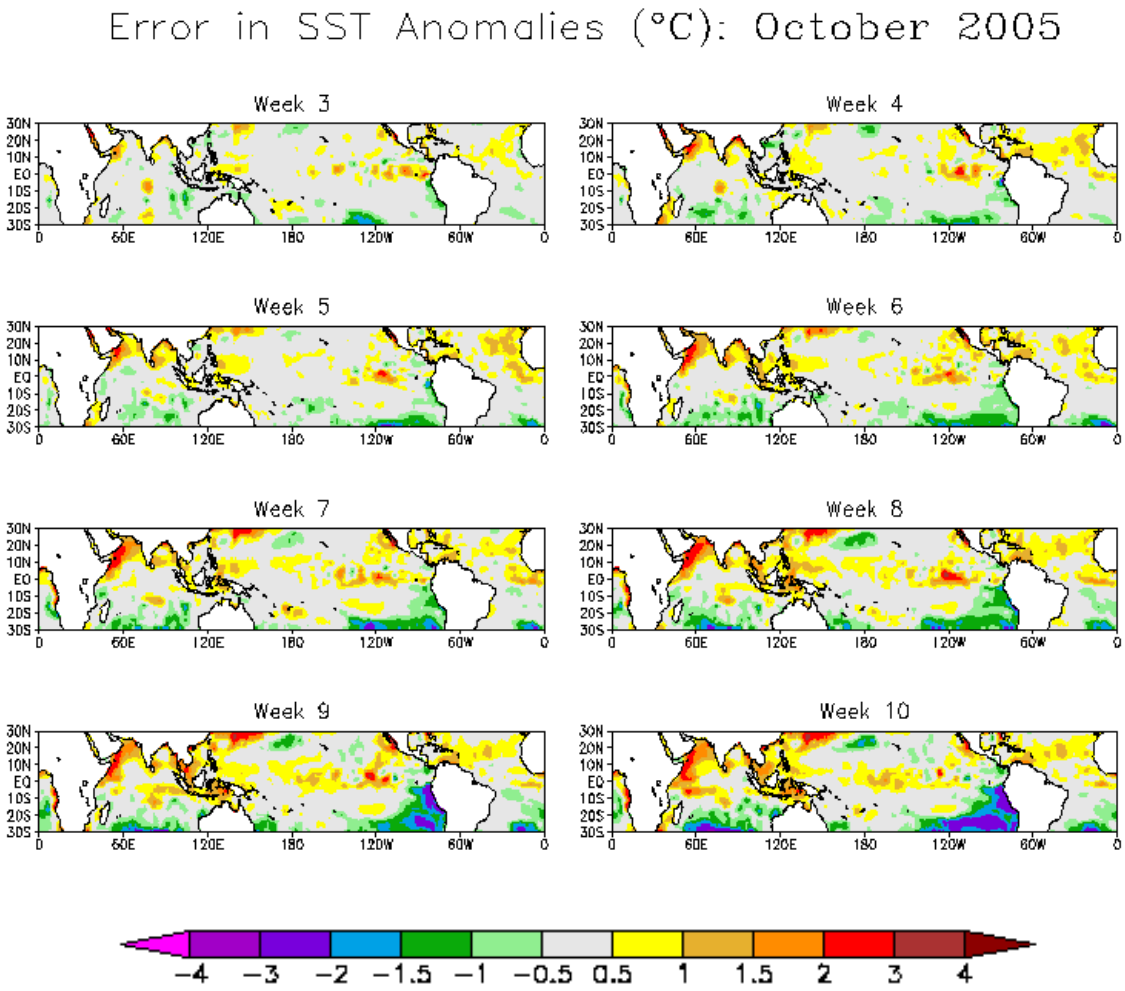

(b)

Figure 1.1 (continued)

CHAPTER 2
DATA AND METHODOLGY

2.1 The Model

The model data used for this study originates from the FSU/COAPS global model. The model is a spectral model run at a T63L17 resolution (roughly 1.875 degrees by 1.875 degrees and seventeen vertical levels) using an Arakawa-Schubert convective scheme (Hogan and Rosmond 1991). In depth details of the model parameterizations can be found in Cocke and LaRow (2000). The global model results are then dynamically downscaled to a 20km by 20km grid over the southeastern United States. The downscaling is performed using the FSU nested regional spectral model (NRSM) (Cocke and LaRow 2000) which uses a perturbation technique to downscale the global data. This method allows for large-scale features simulated by the global model to be passed into the regional domain. Further details and explanations of the dynamical downscaling can be found in Cocke and LaRow (2000).

2.2 Experimental Setup

The global and regional model real-time and hindcast runs from October 2004 and 2005 are used for this study. The real-time runs are integrated out to six months and use a method of persistence to obtain SSTs. The observed SSTA (Reynolds et al. 2002) at the initial time of the forecast is persisted throughout the six month period. Then, for each month of the forecast, the persisted SSTA is added to the long term SST climatology to acquire the full SST field. In order to update the last half of the six month forecast, separate three month forecasts are conducted in January and June using updated SSTA. This study focuses on the wintertime forecasts (December, January, and February) from the October real-time runs because of the known teleconnections between tropical Pacific SSTs and southeastern United States climate during the

winter season (Ropelewski and Halpert 1986; Montroy 1996; Gershunov and Barnett 1997). These forecasts from the real-time runs are then compared to the hindcast runs.

The hindcasts runs used in this study are also integrated in October, resulting in six month forecasts. Weekly updated observed SSTs are used as input to the model versus the persisted SSTA method used when the model was run in real-time. Because there are only three years of October real-time runs, the hindcasts runs from 1987-2005 are used in the study as both real-time and hindcast model climatology.

For both runs, an average of five ensemble members is used to evaluate the model. Using an ensemble prediction system versus a single forecast has several advantages such as: the ability to take into account uncertainty of initial conditions, the ability to examine the atmospheric predictability in a probabilistic framework, and the ability to consider the model's uncertainty in dynamics and physics. The majority of ensembles are created by either varying the initial conditions or perturbing the model physics. The ensemble members used in this study are generated by using time-lagged ECMWF (European Center for Medium range Weather Forecasting) initial conditions for the atmosphere, centered on the first day of the forecast.

2.3 Observations

The observations used in this study come from the National Weather Service's (NWS) Cooperative Observing Program (COOP) Summary of the Day (TD 3200 3210) and were provided by the Florida Climate Center (www.coaps.fsu.edu/climate_center). The dataset merges the NWS's "first order" and "second order" stations. The majority of the data comes from the COOP network, which consists of over 11,000 trained volunteers and has provided over 100 years of climate data throughout the United States. The dataset is maintained and quality controlled by a combination of NWS field representatives, Cooperative Program Managers (CPMs), and hydro-meteorological technicians (HMTs). Further details of the dataset and the COOP observing network can be found from the National Climatic Data Center (NCDC) dataset documentation page (http://www4.ncdc.noaa.gov/ol/documentlibrary/datasets.html).

In this study, daily and monthly precipitation and surface temperature from January 1987 through June 2007 are used to verify the model forecasts. Only long term stations (1948-present)

in Florida, Georgia, and Alabama are used in the analysis (Figure 2.1). In an attempt to eliminate any errors or biases with the observation dataset, the following guidelines are applied: any station missing climate data for a single day is eliminated for that day, the entire month is considered missing if more than tens days in the month are eliminated, and finally, for the climatology, if more than five years of the twenty year climatology are missing, then the station is eliminated from the climatology. Even with these guidelines, observations needed for validation are still available for a large portion of the southeastern United States (Figure 2.2). For each grid point of the model, the closest station's (determined by the great circle distance) temperature and precipitation were assigned to that grid point resulting in an identical 20km by 20km gridded dataset over the southeastern United States as the model (Figure 2.3). Because of the simplicity of this method and the not as simple characteristics of atmospheric variables, there are some disadvantages in using the great circle distance to obtain a gridded dataset. Since temperature is fairly uniform across the southeast, assigning a grid point the closest station's temperature should only be problematic when stations are located in areas of varying terrain (mountains and valley's in northern Alabama and Georgia, major lakes and rivers, or coastal regions). Precipitation, on the other hand, can vary greatly, even across short distances. Using the great circle distance to convert station data to gridded data has its' limitations and should be considered when examining the results.

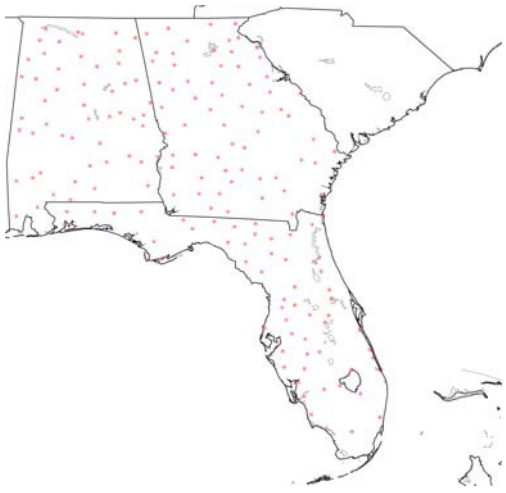

Figure 2.1. Long term stations (1848-present) from the COOP observing network in Florida, Alabama, and Georgia used for model verification.

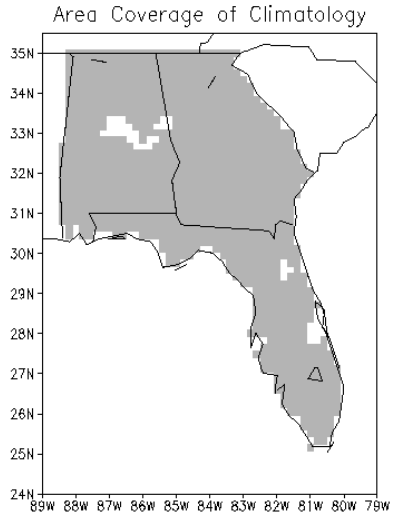

Figure 2.2. Areas of available observation data (lightly shaded) after missing reports were accounted for.

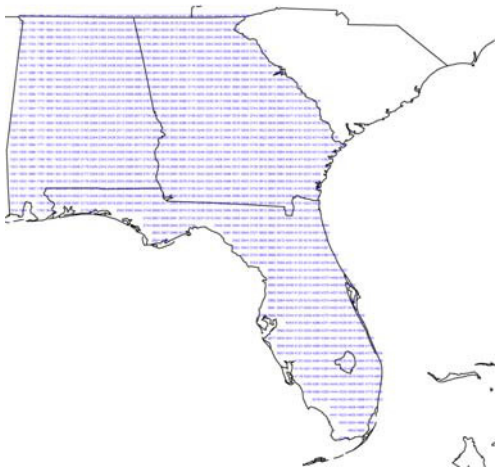

Figure 2.3. Grid points (20 km resolution) of the dynamically downscaled FSU/COAPS NRSM.

CHAPTER 3
RESULTS: MAXIMUM AND MINIMUM TEMPERATURE FORECASTS

3.1 Ensemble Spread, Climatology, and Bias Correction

Once again, for this study an average of five ensemble members is used. Results from the 2004 real-time runs are used as an example to examine the ensemble spread. For maximum and minimum temperature the ensemble spread (the largest difference between two ensemble members) remains small (less than 6˚C) from the initial time of the forecast and through the first fifteen days (Figure 3.1 a and b). After thirty days into the forecast, the ensemble spread is regularly over 10˚C, and the spread reaches a maximum (22˚C for maximum temperature and 28˚C for minimum temperature) at seventy four days into the forecast. Towards the end of the fifth month and into the six month of the forecast, the ensemble spread slightly decreases again. The spread indicates a lack of predictive skill out past ten days and the need to rely on probabilistic scoring for climate studies. For each individual day, the ensemble average does not always result in the most accurate forecast, especially for anomalous cold or warm periods. However, the ensemble average is still used to validate the model due to the known positive results in ensemble forecasting (Palmer 1993; Tracton and Kalnay 1993).

In comparison to observations, a forecast of the ensemble average (heavy black line) consistently underestimates both maximum and minimum temperature (Figure 3.1 a and b). Forecast models tend to have biases of some kind or another, referred to as systematic errors. Comparing the nineteen year hindcast model climatology to the nineteen year observed climatology highlights the FSU/COAPS NRSM systematic error in maximum and minimum temperature (Figure 3.2 a and b), given perfect observed SSTs. The difference in climatologies shows evidence of a -1˚C to -6˚C cold bias in both maximum and minimum temperature for the winter months (DJF) in the southeast. The cold bias is most noticeable in January and less extreme in December and February. On average, central Florida through southern Georgia show the strongest maximum temperature bias, while for minimum temperature the strongest cold bias

tends to be in central Georgia and Alabama. The cold bias in Georgia and Alabama have been noted in other studies using the FSU/COAPS NRSM (Shin et al. 2005). In order to account for these systematic errors, the model data is bias corrected after the model run but before validation.

In an attempt to account for the model's maximum and minimum surface land temperature biases, the following bias correction method is performed:

$$T_{bc} = (T_m - \overline{T}_m) + \overline{T}_o$$

where T_m is the model forecasted maximum(minimum) daily temperature, $\overline{T}_m$ is the model's monthly maximum(minimum) temperature climatology, and $\overline{T}_o$ is the observed monthly maximum(minimum) climatology. Ideally, bias correction on the daily model output would be performed using nineteen year daily climatology. Nineteen year daily model climatology is not currently available, but since daily model data still needs to be evaluated for crop model input, monthly observed and model climatology is used for bias correction. Again, the hindcast climatology is used to bias correct both the hindcast and real-time runs because only three years of real-time runs are available. Using the 2004 real-time runs as an example, the bias correction slightly reduces the cold bias in maximum and minimum temperature, decreasing the model systematic error (Figure 3.3 and 3.4). Now that the model data is bias corrected, the model's ability to forecast temperature can be examined. For the remainder of this section, bias corrected model output is used to verify the model, unless verifying anomalies, in which the systematic error is already accounted for by using the model or observed climatologies to calculate the anomalies.

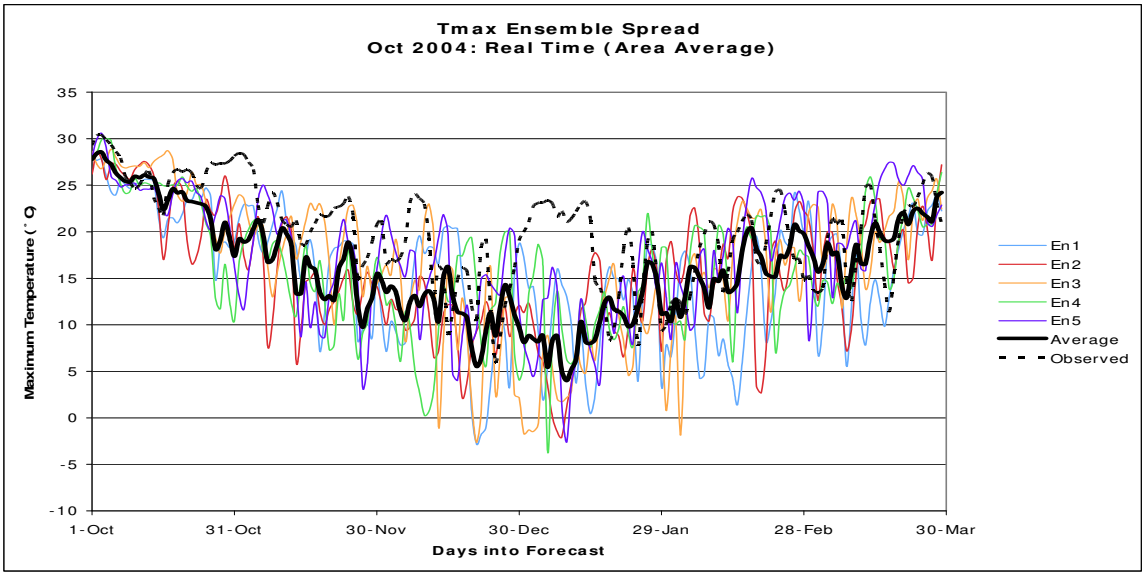

(a)

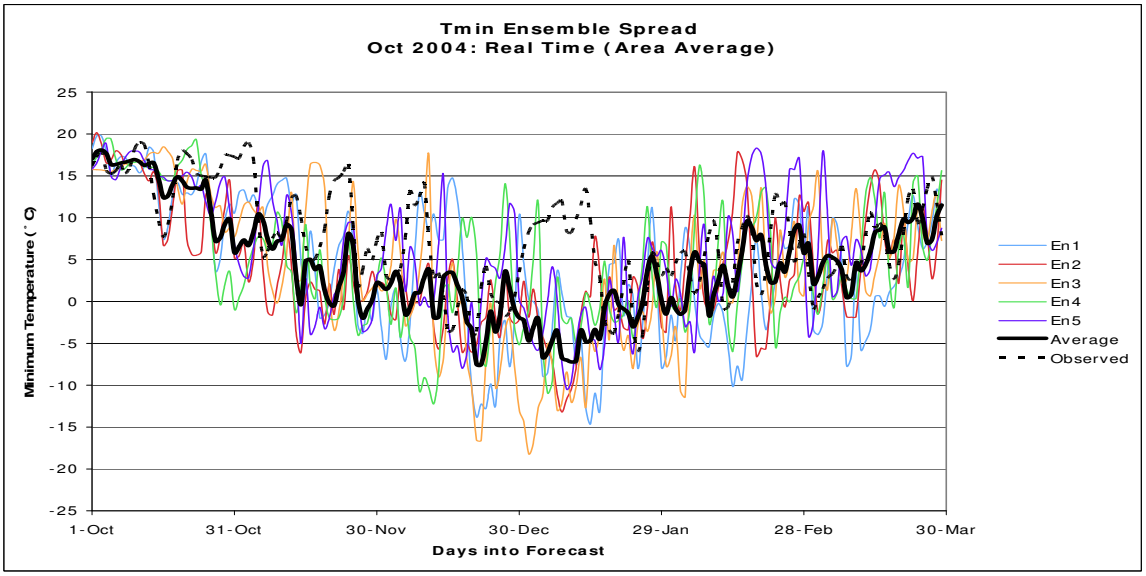

(b)

Figure 3.1. Daily maximum (a) and minimum (b) temperature model output and observations from the October 2004 real-time runs area averaged over Florida, Georgia, and Alabama. The chart displays output for all five individual ensemble members (blue, red, orange, green, and purple), the ensemble average (black bold), and what was observed (black dashed).

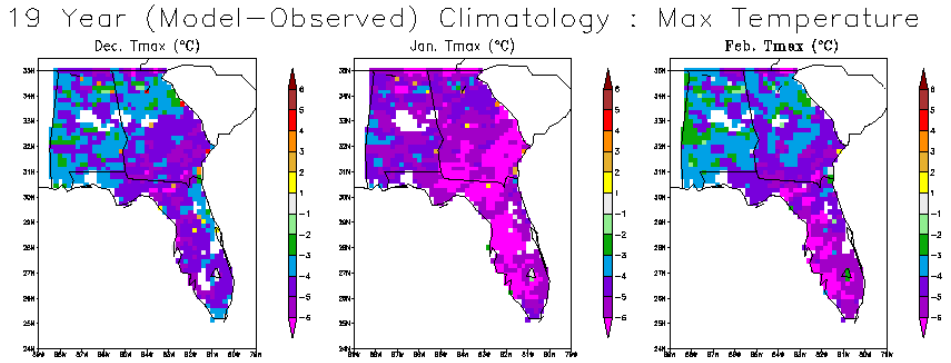

(a)

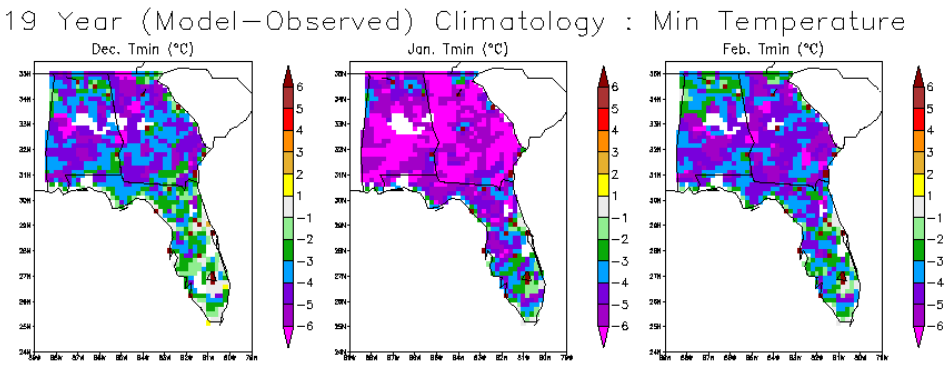

(b)

Figure 3.2. The difference between the nineteen year monthly model climatology and the 19 year monthly observed climatology for maximum (a) and minimum (b) temperature in December (left), January (center), and February (right). The model climatology originates from nineteen years of October hindcasts runs.

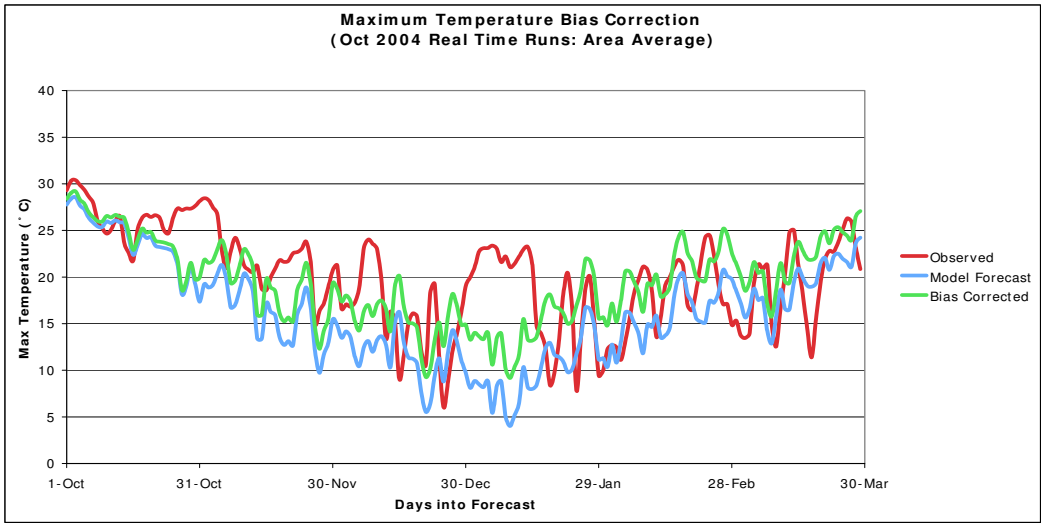

(a)

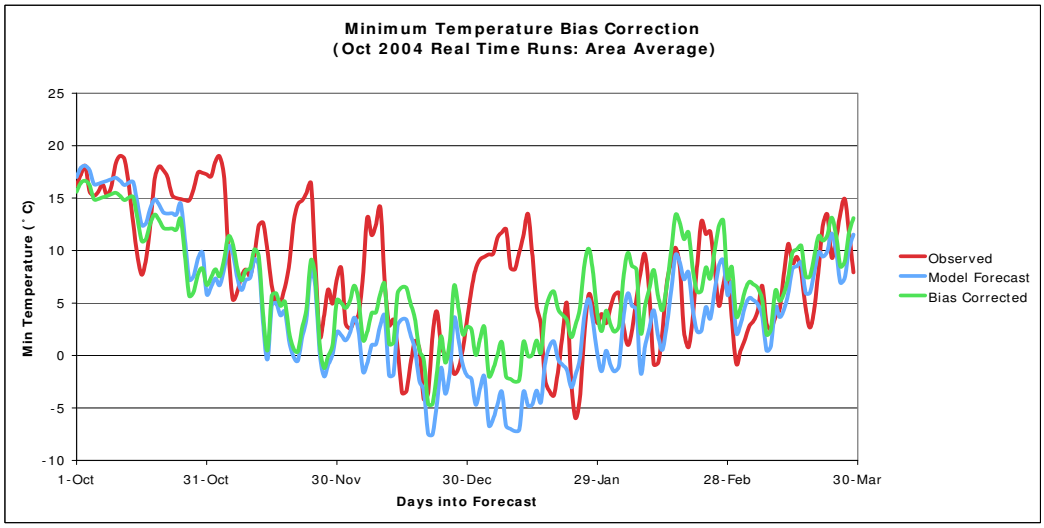

(b)

Figure 3.3. Daily maximum (a) and minimum (b) temperature output from the October 2004 real-time model runs (blue), the October 2004 bias corrected real-time runs (green), and what was observed (red) area averaged over Georgia, Alabama, and Florida.

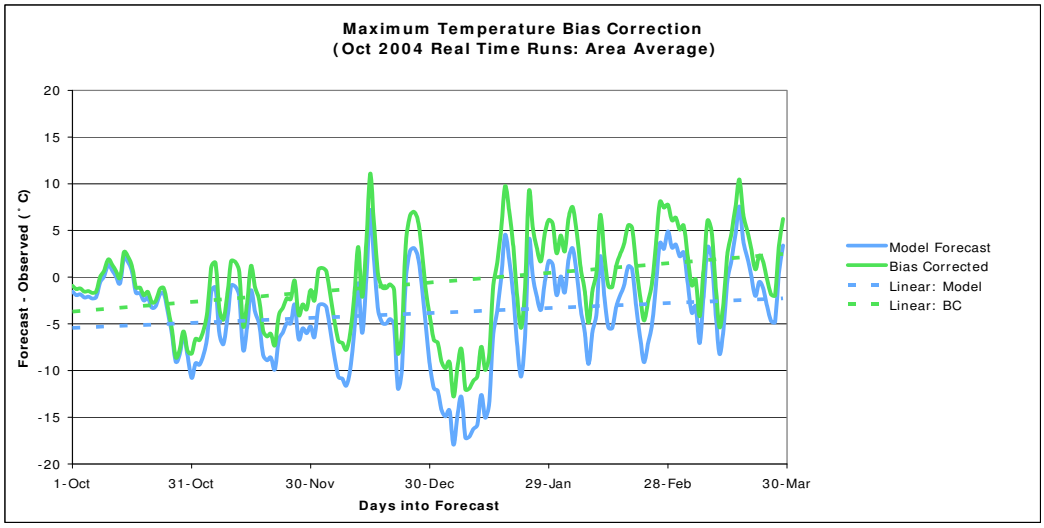

(a)

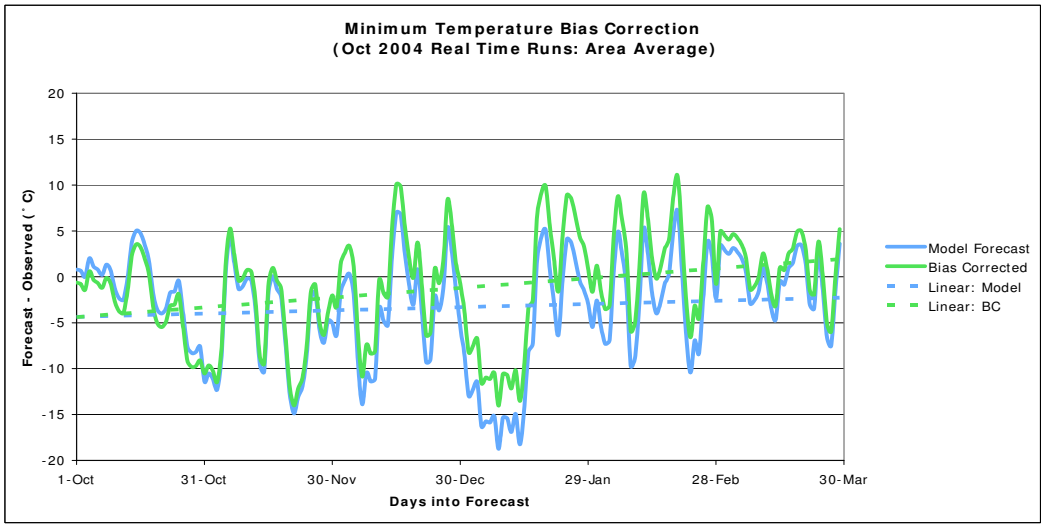

(b)

Figure 3.4. Area averaged (over Georgia, Alabama, and Florida) daily maximum (a) and minimum (b) forecasted temperature minus the area averaged observed temperature from the October 2004 real-time runs (solid blue) and October 2004 bias corrected real-time runs (solid green). A line of linear fit is also plotted for both the raw forecast (dashed blue) and bias corrected forecast (dashed green).

3.2 Seasonal/Monthly Predictions

To evaluate the model's ability to forecast seasonal and monthly maximum and minimum temperature anomalies across the southeast, the observed and model anomalies are determined:

$$\text{anomaly} = (T_m - \overline{T}_m)$$

where T_m is the forecasted(observed) temperature and $\overline{T}_m$ is the model(observed) climatology. For a specific example, to calculate the model's seasonal maximum temperature anomaly T_m is the daily forecasted maximum temperatures averaged over a three month season, and $\overline{T}_m$ is the nineteen year monthly model climatology of maximum temperature averaged over a three month season.

Spatial plots of the error in seasonal forecasts show that the model is generally capable of predicting the wintertime (DJF, two month lead time) maximum and minimum temperature anomalies for both the 2004 and 2005 seasons. The majority of the temperature anomaly errors stay under 3˚C (Figure 3.5). Observations indicate that near neutral (less than 1°C anomaly) conditions prevailed in the southeast in both 2004 and 2005, with mostly positive anomalies (0-2˚C) in Alabama and into northern Georgia and slightly negative anomalies in southern Florida. The DJF forecasts from the October 2004 real-time runs correctly forecast near normal (less than 1°C anomaly) maximum and minimum temperatures for most of the southeast. However, the model incorrectly predicts the smaller (cooler) anomalies to be in northern Alabama and Georgia and the larger (warmer) anomalies to occur in Florida (Figure 3.5 a and c). The DJF forecasts from the October 2005 real-time runs accurately capture the cooler maximum temperature anomalies to be in the south, and it predicts positive anomalies (0-3°C) for the entire southeast, resulting in 0-2°C errors for most of the area (Figure 3.5 b and d). When comparing the real-time runs to the hindcasts runs, the 2005 DJF seasonal forecasts looked fairly similar for both maximum and minimum temperature. Both real-time and hindcast runs forecast warm anomalies throughout the southeast, but the hindcast run predict less of a warm anomaly resulting in less error (0-1°C) than the real-time forecasts (1-3°C). In 2004, the maximum and minimum temperature forecasts from the real-time and hindcast runs are also similar. Both runs incorrectly forecast cooler anomalies in northern Alabama and Georgia and warmer anomalies to the south. The 2004 hindcast runs show larger errors (greater than 3°C) than the 2004 real-time runs (mostly less than 3°C of error) in the north because of the strong positive anomalies in Alabama and Georgia, but the 2004 hindcast runs have smaller errors (less than 1°C) than the 2004 real-time runs (1-2°C) in southern Florida. The magnitude of error in the real-time runs between

maximum and minimum temperature are comparable in 2004, but in 2005 the model produces larger errors in minimum temperature.

In order to easily compare the real-time and hindcast model statistics, Taylor diagrams are created. Taylor diagrams provide a means of determining the statistical relationship between what is forecasted and what is observed (Taylor, 2001). The original Taylor diagram plots the correlation, centered root-mean square difference, and standard deviation to summarize how closely a forecast pattern matches observations. The Taylor diagrams used in this study are a modified version. This version normalizes the standard deviation of the model forecast by the observed standard deviation, which allows for model statistics from both 2004 and 2005 to be plotted on the same diagram (See Appendix A, page 66). For these modified Taylor diagrams, a mark is made for each model run, which represents the correlation, normalized standard deviation, and centered root mean squared (RMS) difference. The closer the mark lies to the square "reference" mark on the plot, the closer the forecast temperature pattern matches the observed.

Strictly considering Taylor diagram model statistics, both the 2005 real-time and hindcast runs outperform the 2004 model runs in forecasting maximum and minimum temperature (Figure 3.6 a and b). The real-time correlation and standard deviation values tend to cluster around the hindcast values in 2004 and 2005, indicating no significant difference between real-time and hindcast model performance for wintertime forecasts. For both 2004 and 2005 DJF forecasts, the real-time runs have higher correlation values than the hindcast runs, while the hindcast runs have standard deviation values closer to what was observed. When comparing the real-time and hindcast model output to a forecast of climatology, climatology outperforms the models in 2004 in terms of correlation, standard deviation, and RMS values. In 2005, the model forecasts have similar or even better forecasts then climatology.

The model's ability to predict monthly anomalies for December (two month lead time), January (three month lead time), and February (four month lead time) is also examined. For the October 2004 real-time model runs, the December and February maximum and minimum temperature forecasts are similar to the October 2004 real-time seasonal forecasts with positive (1-3°C) errors in Florida and neutral to negative (0-$^{-}$2°C) errors in northern Georgia and Alabama (Figure 3.7 a and c). In January, the model forecasts cooler anomalies than what was observed, resulting in anomaly errors greater that -6°C in northern Alabama, as well as large

negative errors in the rest of Alabama and throughout Georgia. The December and February temperature anomaly patterns from the 2005 real-time model runs are also similar to the seasonal forecast with positive anomalies for most of the southeast, but the February forecasts is a littler warmer than observations, resulting in up to 5°C anomaly errors in northern Alabama (Figure 3.7 b and d). Like the 2004 real-time model runs, the January forecast from the 2005 real-time runs underestimates maximum temperature for most of Alabama and Georgia. In general, the real-time runs have comparable or even smaller temperature anomaly errors than the hindcast runs (Figure 3.7 a-d). For both years, the hindcast runs under predicts maximum and minimum temperature for January, with errors greater than -6°C in 2004. Also, for both years the hindcast runs over predict December maximum and minimum temperatures, especially for the 2005 model runs. The January 2004 cold bias and the December 2005 warm bias appear stronger in the minimum temperature forecasts.

Once again, Taylor diagrams are created in order to easily compare the model's correlation, standard deviation, and RMS values (Figure 3.8 a-f). Similar to the seasonal forecasts, the 2005 monthly forecasts tend to outperform the 2004 forecasts in terms of correlation and standard deviation. This is especially true when considering the standard deviations. Also like the seasonal forecasts, the real-time runs generally have higher correlations (values closer to one) compared to the hindcast runs, while the hindcasts runs usually have standard deviations closer to what was observed. As expected from previously examining the spatial plots of errors in monthly anomalies, the January forecasts of maximum and minimum temperature show little skill compared to the February and December forecasts. When comparing the real-time and hindcast model output to a forecast of climatology, climatology tends to outperform the models in 2004, but is similar to both 2005 model forecasts.

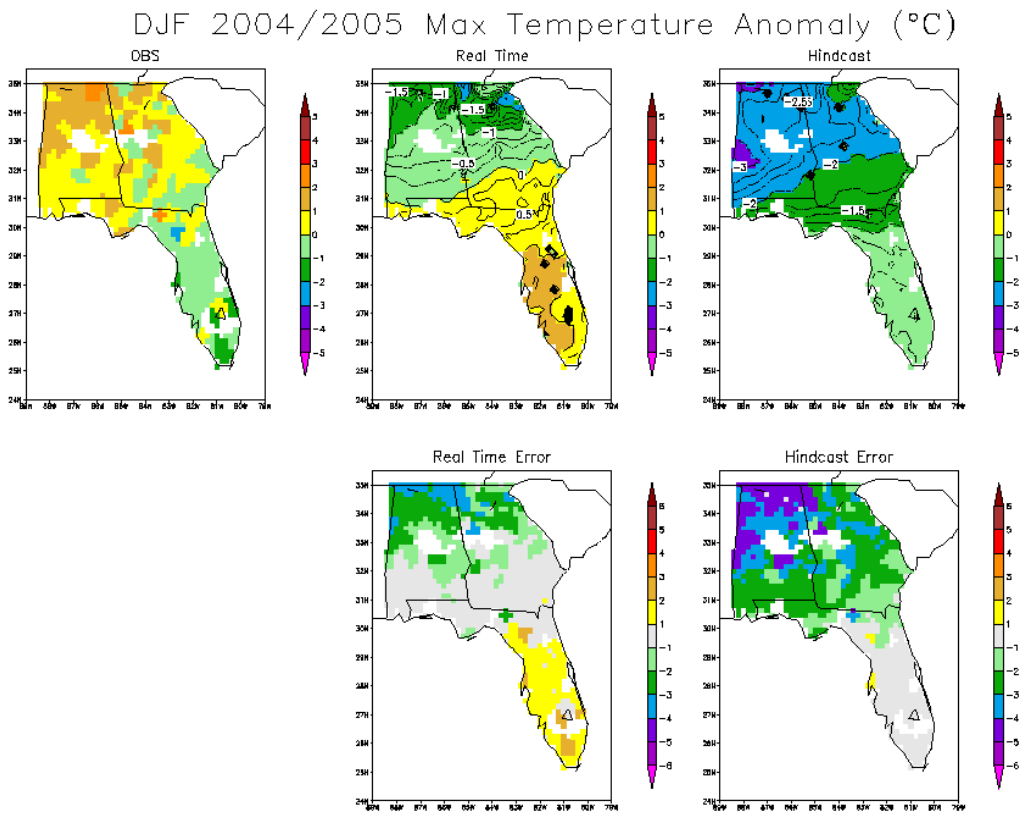

(a)

Figure 3.5. Spatial plots of the DJF 2004/2005 and DJF 2005/2006 maximum temperature (a and b), and DJF 2004/2005 and DJF 2005/2006 minimum temperature (c and d). Each group of figures plot the observed anomaly (top left), the real-time run anomaly (top center), the hindcast run anomaly (top right), the real-time run anomaly minus the observed anomaly (bottom center), and the hindcast run anomaly minus the observed anomaly.

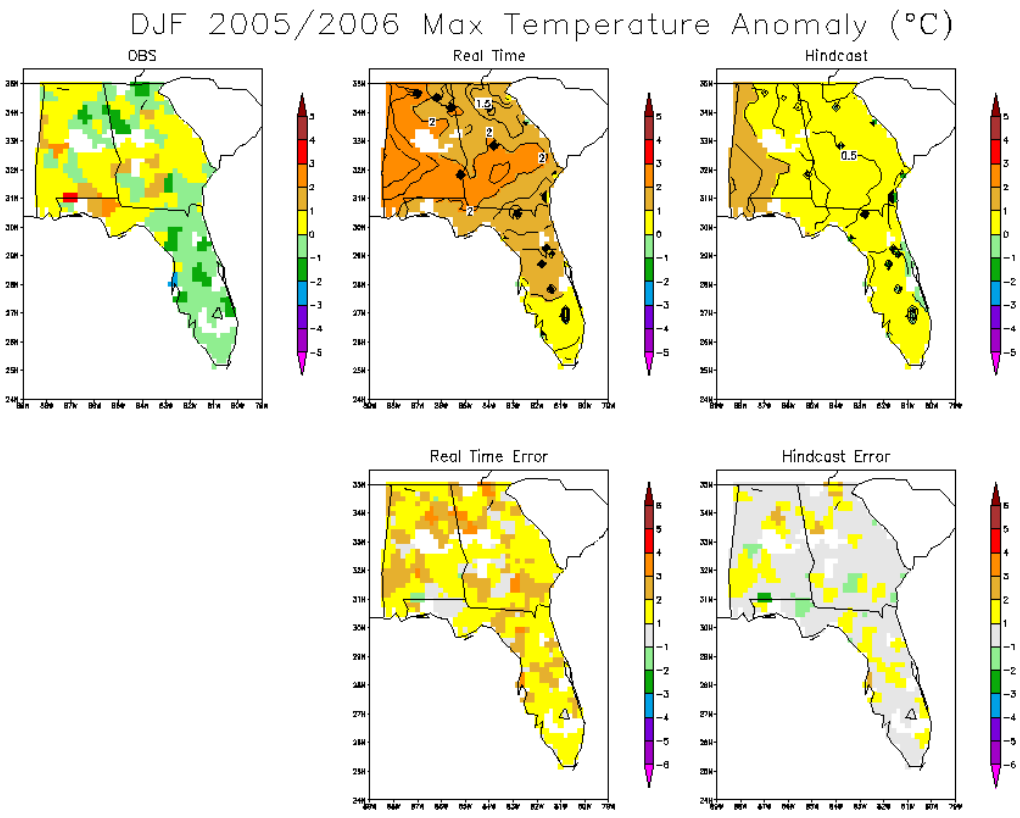

(b)

Figure 3.5 (continued)

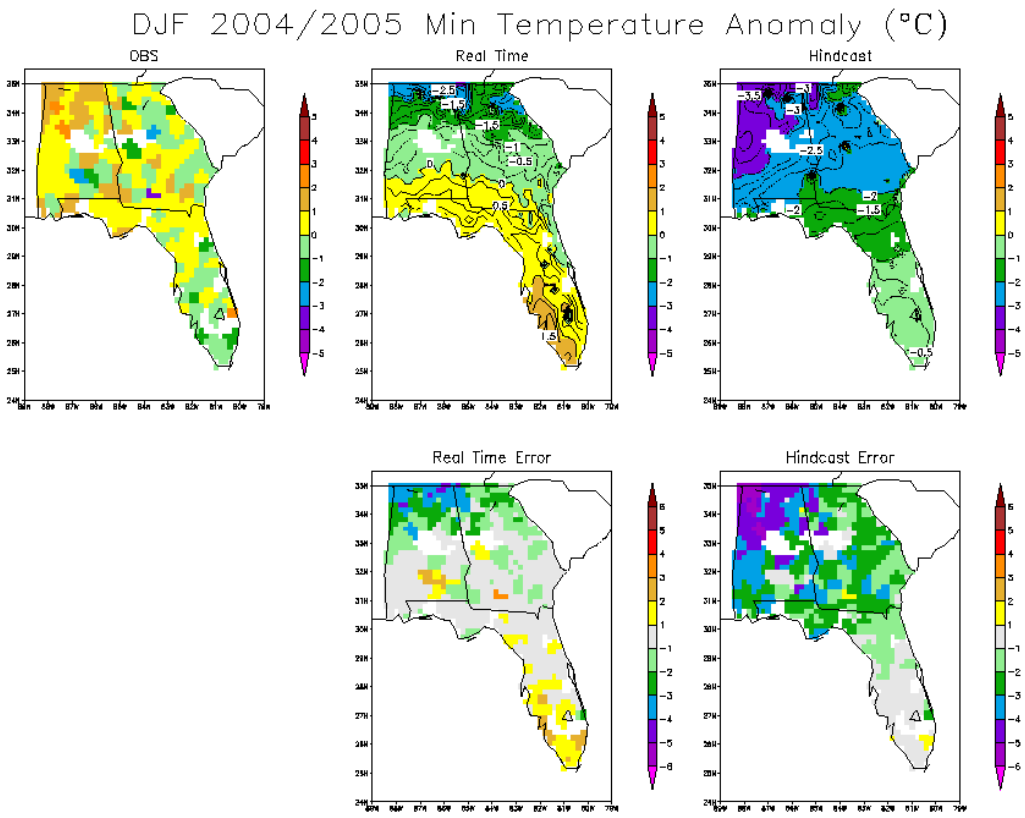

(c)

Figure 3.5 (continued)

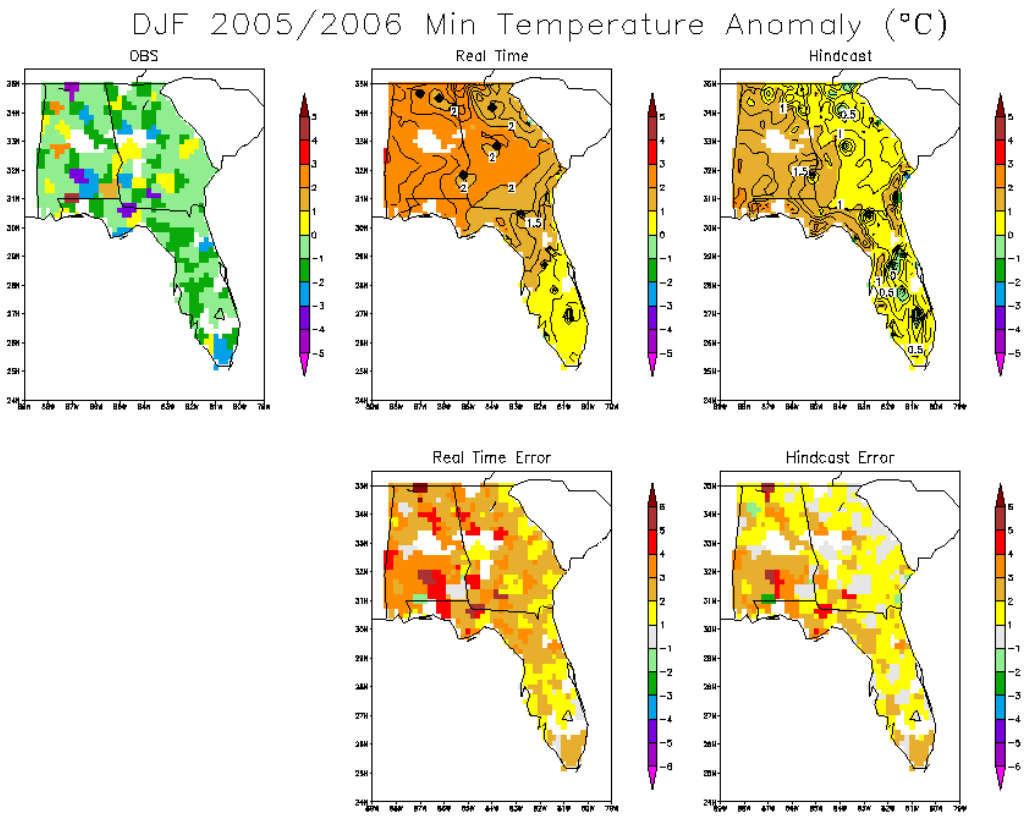

(d)

Figure 3.5 (continued)

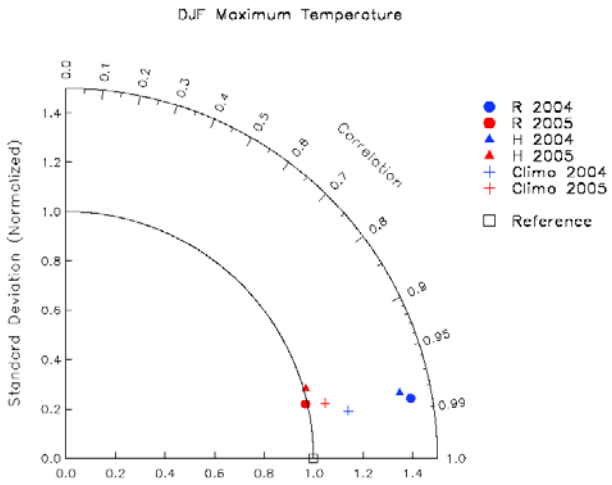

(a)

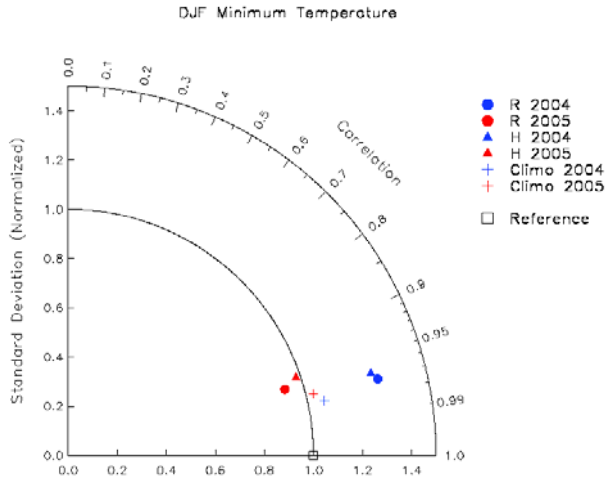

(b)

Figure 3.6. Taylor diagrams of the DJF maximum (a) and minimum (b) temperature forecasts. The plots include results from the 2004 real-time runs (blue circles), 2005 real-time runs (red circles), 2004 hindcast runs (blue triangles), 2005 hindcast runs (red triangles), 2004 climatology forecast (blue crosses), 2005 climatology forecast (red crosses), and a perfect forecast reference point (black squares).

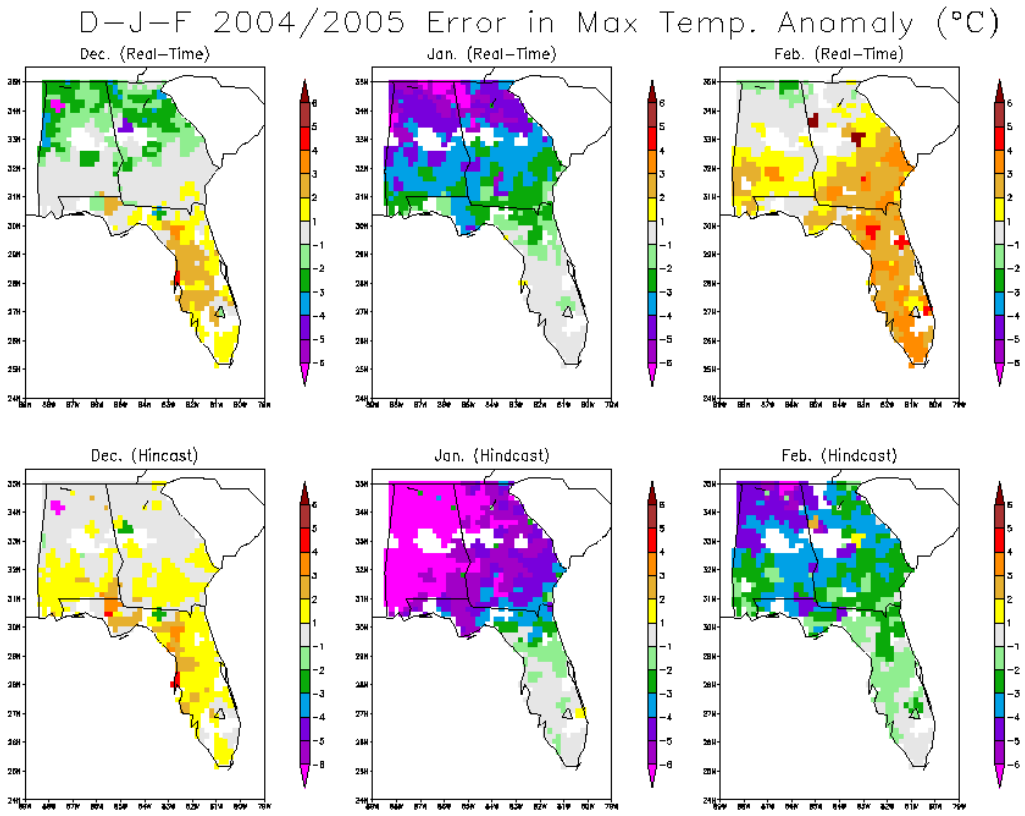

(a)

Figure 3.7. The model forecasted minus the observed monthly anomalies (model error) for December, January, and February (two, three, and four month lead times) 2004/2005 maximum temperature (a), 2005/2006 maximum temperature (b), 2004/2005 minimum temperature (c), and 2005/2006 minimum temperature (d). Each figure has error results from the real-time runs (top row) and hindcast runs (bottom row) monthly anomaly forecasts from December (left), January (center), and February (right).

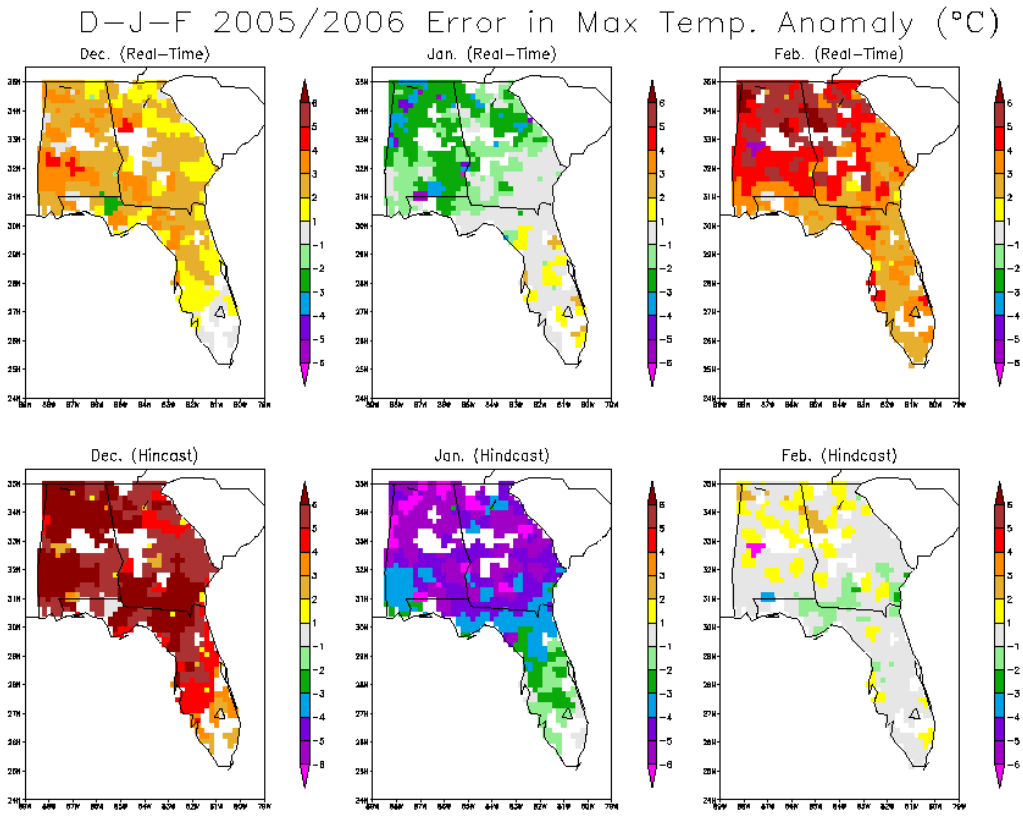

(b)

Figure 3.7 (Continued)

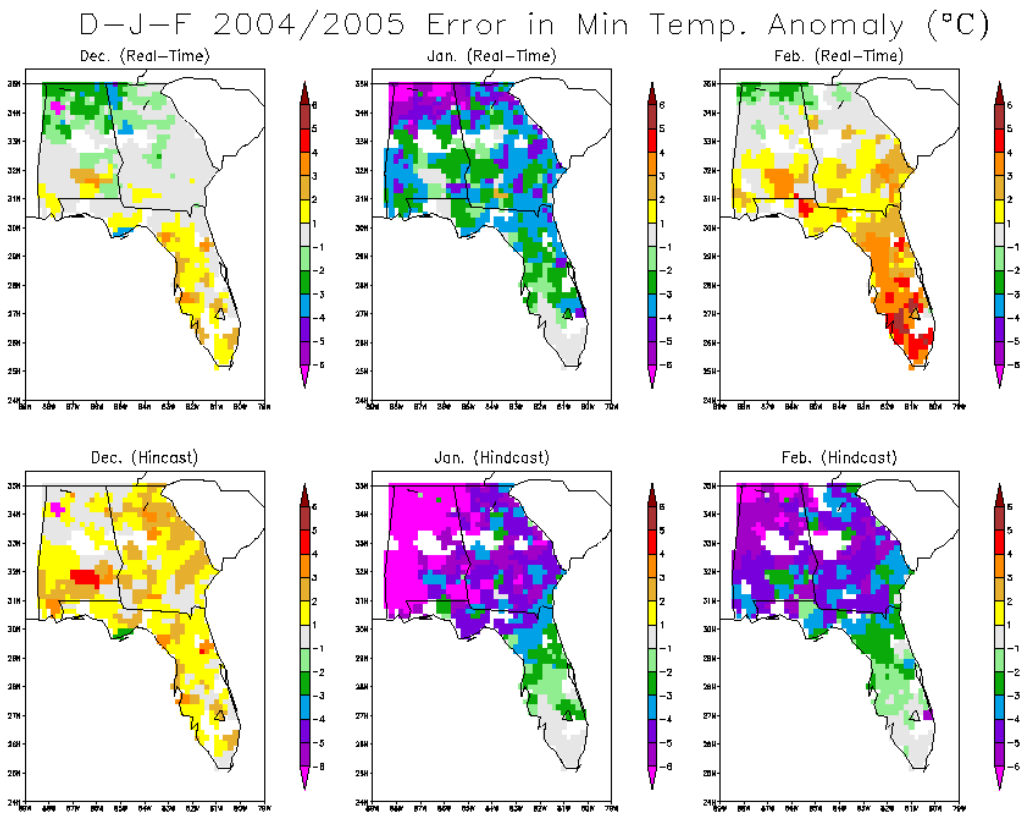

(c)

Figure 3.7 (Continued)

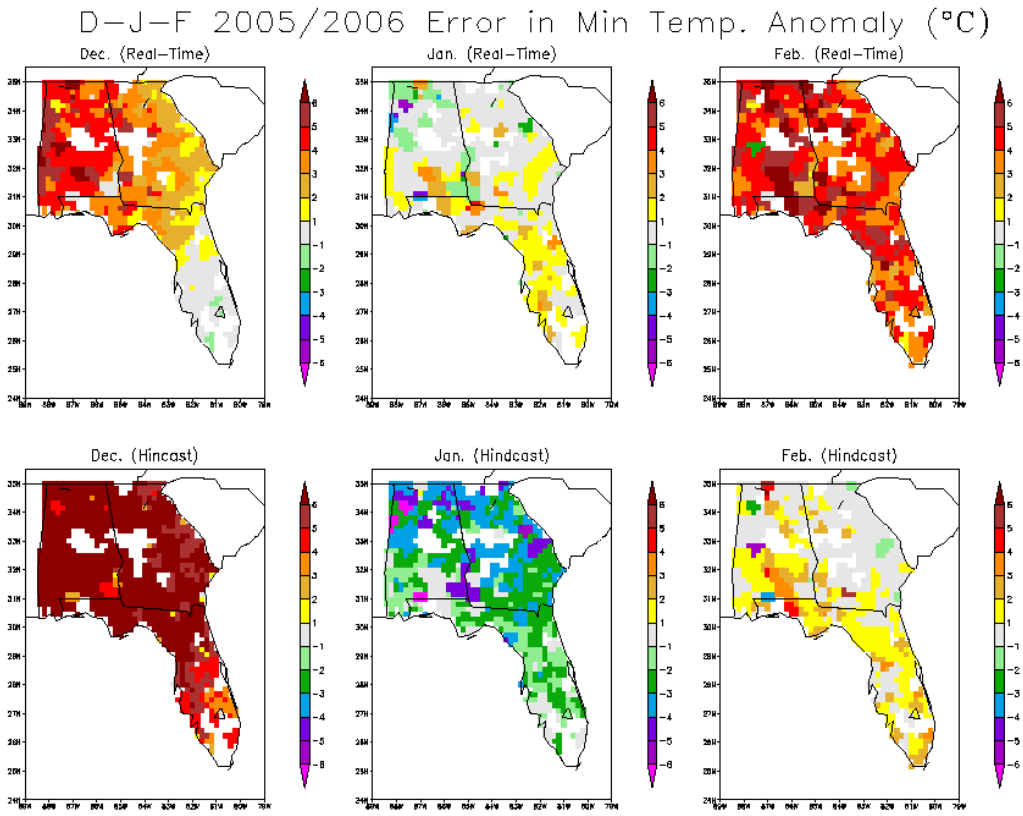

(d)

Figure 3.7 (Continued)

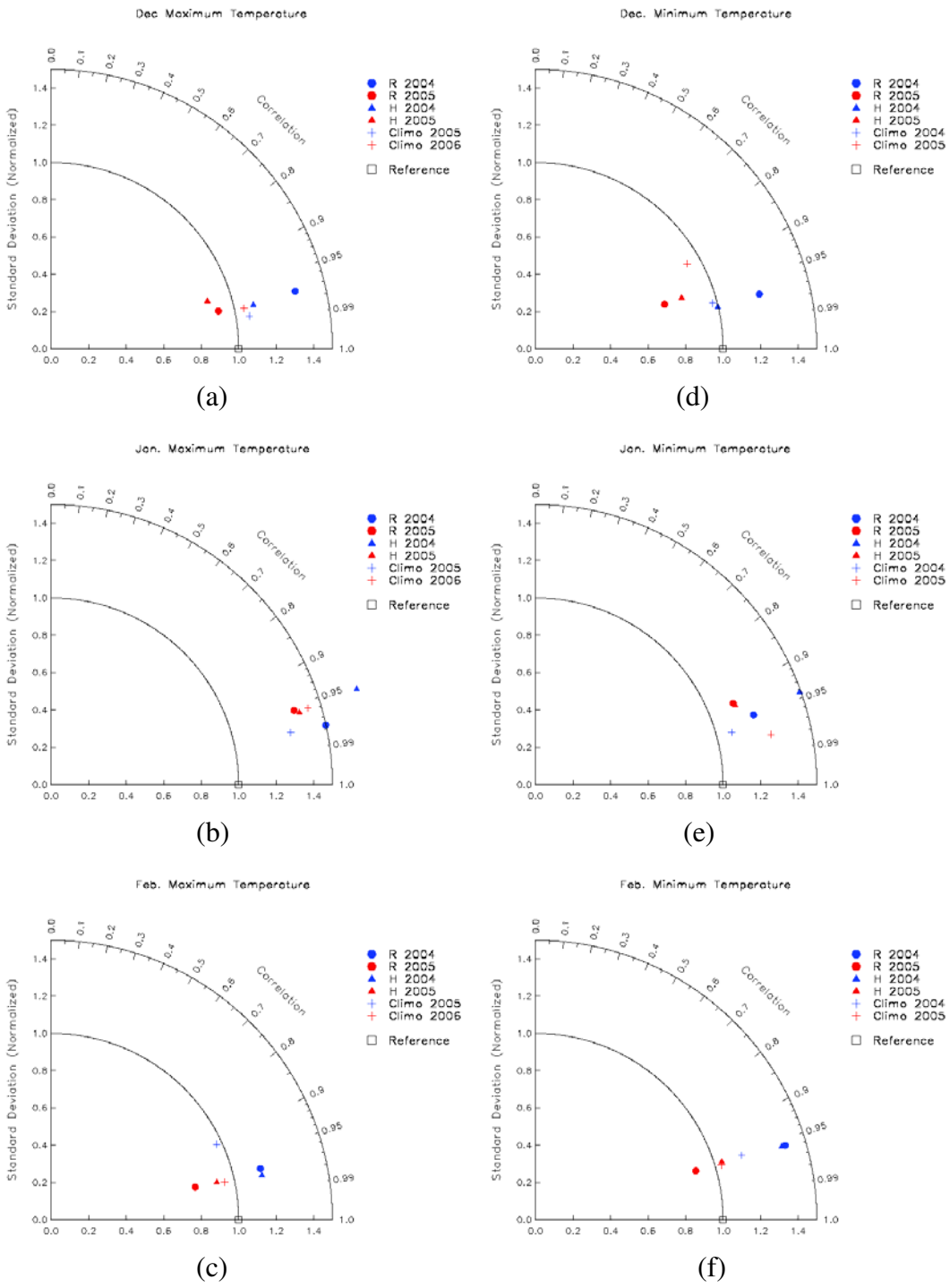

Figure 3.8. Taylor diagrams from the December, January, and February maximum (a,b, and c) and minimum (d,e, and f) temperature forecasts. The plots include results from the 2004 real-time runs (blue circles), 2005 real-time runs (red circles), 2004 hindcast runs (blue triangles), 2005 hindcast runs (red triangles), 2004 climatology forecast (blue crosses), 2005 climatology forecast (red crosses), and a perfect forecast reference point (black squares).

3.3 Skill Scores and Standard Verification Methods

Skill scores and other standard verification methods are discussed for the DJF seasonal forecast to provide more insight as to how well the model performs and also to easily compare the FSU/COAPS climate model's performance to other climate models. One of the most common measures of verification is the root mean square error (RMSE). It is an easy way to determine the average magnitude of forecast error, but because of its simplicity, it does not offer much value as to why or where the model has errors (Wilks, 307-311). The Brier score (BS) also measures the magnitude of forecast error, but calculates errors of a probability forecast, which uses the ensemble members to determine the probability for various temperature anomaly thresholds (Wilkes, 284-285). The BS does have its limitations. It does not take into the effect of the climatological frequency of an event and therefore leads to deceivingly high skill for infrequent events. Because of this limitation with the BS, relative operating characteristic (ROC) curves and equitable threat scores (ETS) are also evaluated. ROC curves and ETS both take into account the frequency of an event by using results from a contingency table. ROC curves are simply a plot of the probability of detection vs. the false alarm rate and it determines the model's ability to distinguish between events and non-events (Wilks, 294-298). ETS measures the fraction of correctly forecasted observed events, accounting for hits due to random chance (Wilks, 266-267). The ROC curves and ETS also have their limitations. ROC curves are not sensitive to any model bias, which means a poor forecast can still produce a good ROC curve, and an ETS can not distinguish whether forecast error is due to misses or false alarms because they are accounted for in the same manor. Despite the limitations of these verification techniques, they are all still used to examine the predictability of the model.

Considering the RMSE, BS, ROC curves, and ETS (for calculations see Appendix B, page 67), the real-time runs tend to perform better in 2004 than in 2005, while the hindcast runs' results vary for different metrics. Out of the four model experiments examined, the 2005 hindcast runs generally produce the best forecast in terms of skill scores and these standard verification methods, with a maximum temperature RMSE value of only 0.930 °C (Table 3.1) and maximum temperature BS scores closest to 0 (Figure 3.9 a and b). However, the ROC curves do not strongly suggest one forecasts outperforms another. The ability for the models to

distinguish between events and non-events varies for each threat threshold and model run. The ROC curves for both maximum and minimum temperature from the 2004 real-time runs indicate slight skill in determining neutral events, but then the curves fall below the line of no skill for positive and negative 1°C anomaly threats (Figures 3.10 a-e). ETS scores for both maximum and minimum temperature are similar (Figure 3.11 a and b). The majority of ETS scores fell below or near the line of no skill, with the exception of the 2004 hindcast and real-time runs which indicate some skill for a -1°C and 0°C anomaly, respectively. All four verification methods indicate the models shows more skill in forecasting surface maximum temperature than minimum temperature, which agrees with the results from the monthly and seasonal anomaly forecasts.

In an attempt to show how the model compares to another climate forecast method, the BS scores from a reference forecast is plotted. The reference forecast is created from the nineteen years of observation data. A forecast using previous observations usually produces a lower BS score than either the real-time or hindcasts runs, but both the 2004 and 2005 hindcast runs fall only slightly below the BS scores of the reference, indicating, as was found in the previous section that a forecast based on climate data is still difficult to surpass. The BS, ROC curves, and ETS all examine the models ability to forecast temperature for various threat thresholds. The models do not appear to have any distinct pattern of predicting certain threats better than other. For example, the BS plots shows that the 2005 models runs have difficulty in predicting -1°C anomalies, but then in the 2004 runs, the model's skill is reasonable with a BS score close to the reference forecast. Again, each of these methods of verification has their limitations and these limitations should be considered when evaluating the model forecasts.

Table 3.1. RMSE values for the seasonal (DJF) maximum and minimum temperature anomaly forecasts from the October 2004 and 2005 model runs.

	RMSE: DJF Temperature Anomaly			
	Max. T (˚C)		**Min. T (˚C)**	
	2004	**2005**	**2004**	**2005**
Real-Time	1.63	1.89	1.54	2.89
Hindcast	2.65	0.93	2.68	2.08

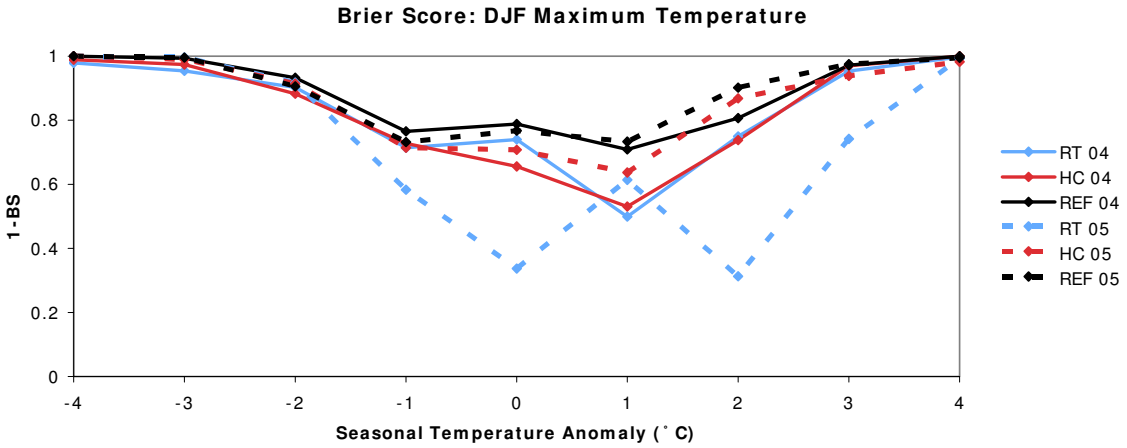

(a)

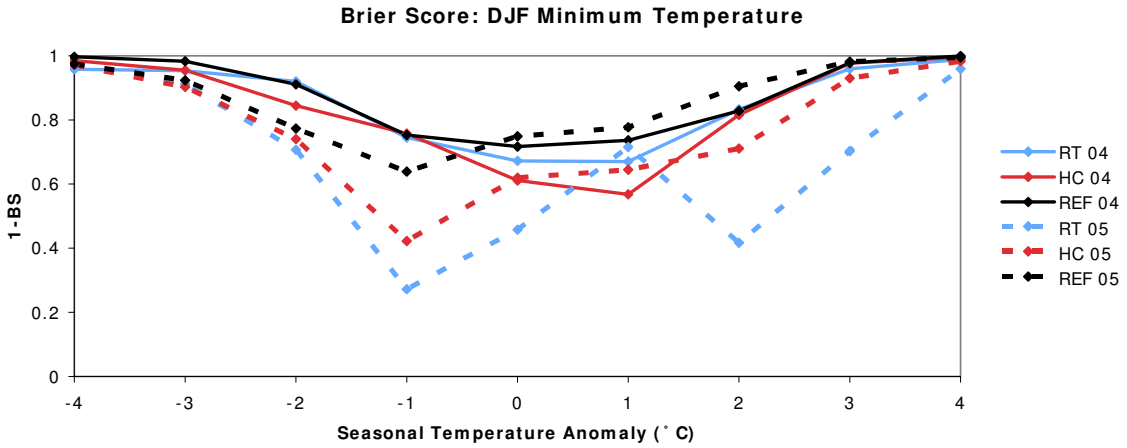

(b)

Figure 3.9. BS for the seasonal (DJF) maximum (a) and minimum (b) forecasted temperature anomalies. Each figure plots scores from the 2004 real-time run (solid blue), 2004 hindcast run (solid red), a 2004 reference forecast (solid black), 2005 real-time run (dashed blue), 2005 hindcast run (dashed red), and a 2005 reference forecast (dashed black).

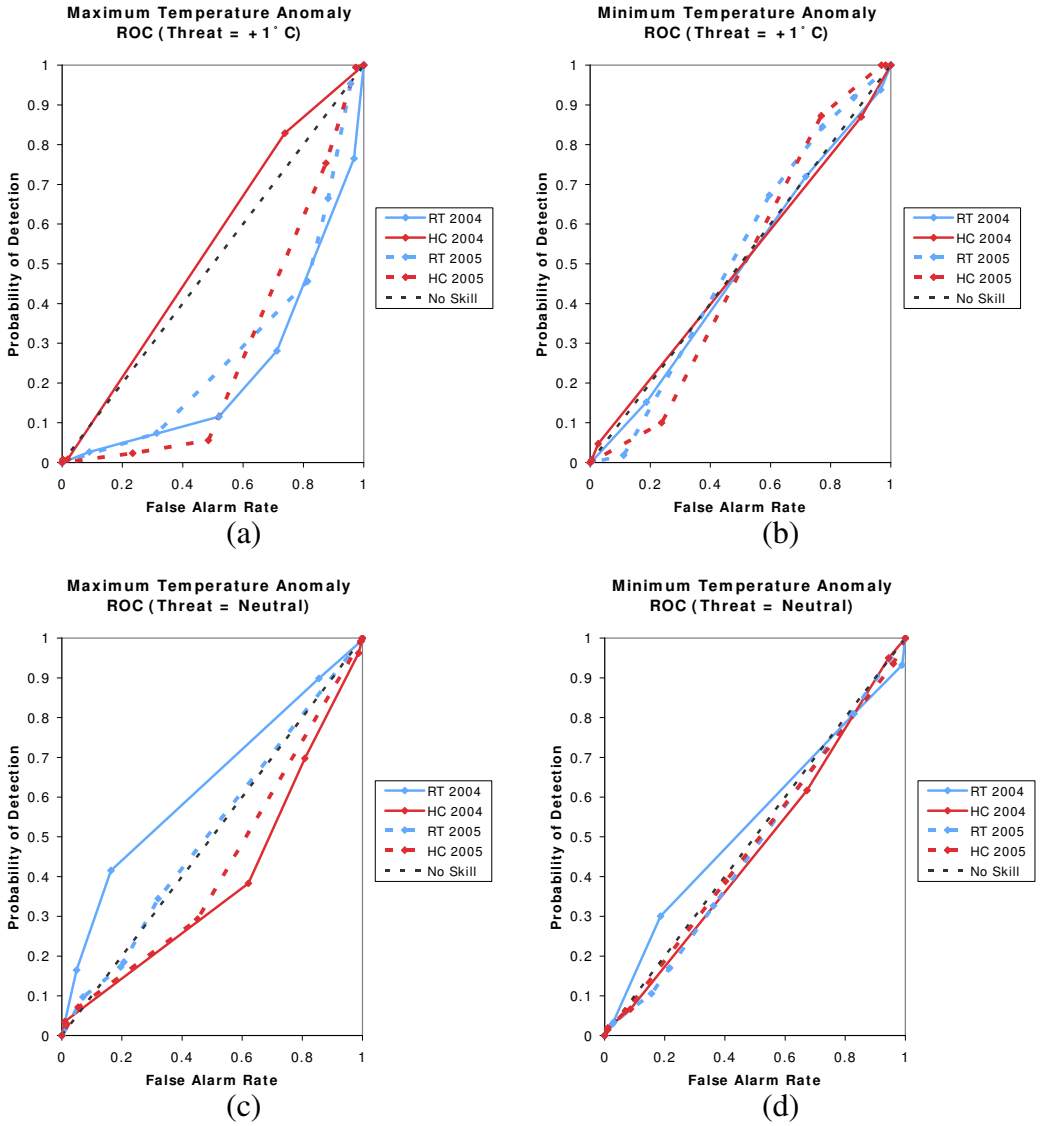

Figure 3.10. ROC curves for maximum and minimum temperature anomalies for a positive 1°C (a and b), neutral (c and d), and negative 1°C (e and f) threshold. Each figure plots curves representing the 2004 real-time runs (solid blue), 2004 hindcast runs (solid red), 2005 real-time runs (dashed blue), 2005 hindcast runs (dashed red), and a line of no skill (dashed black).

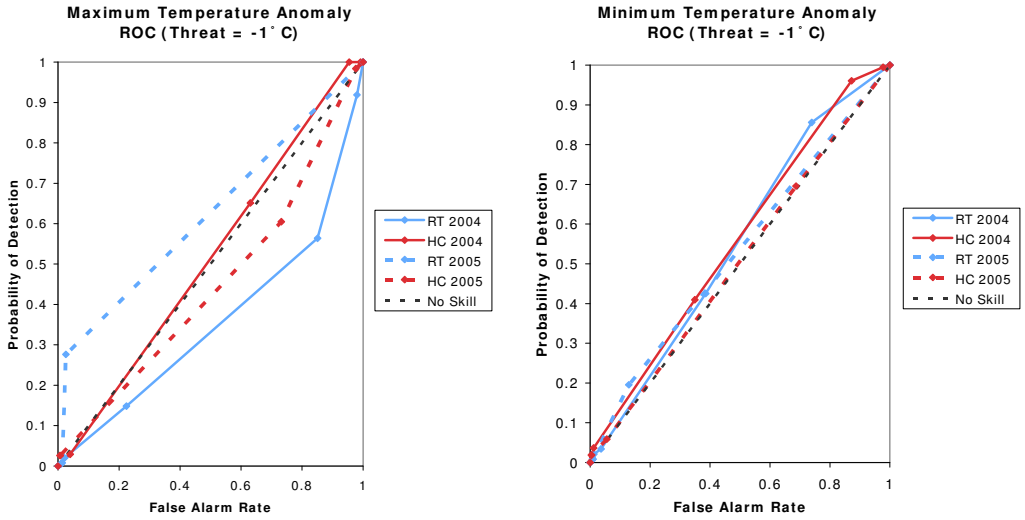

(e) (f)

Figure 3.10 (Continued)

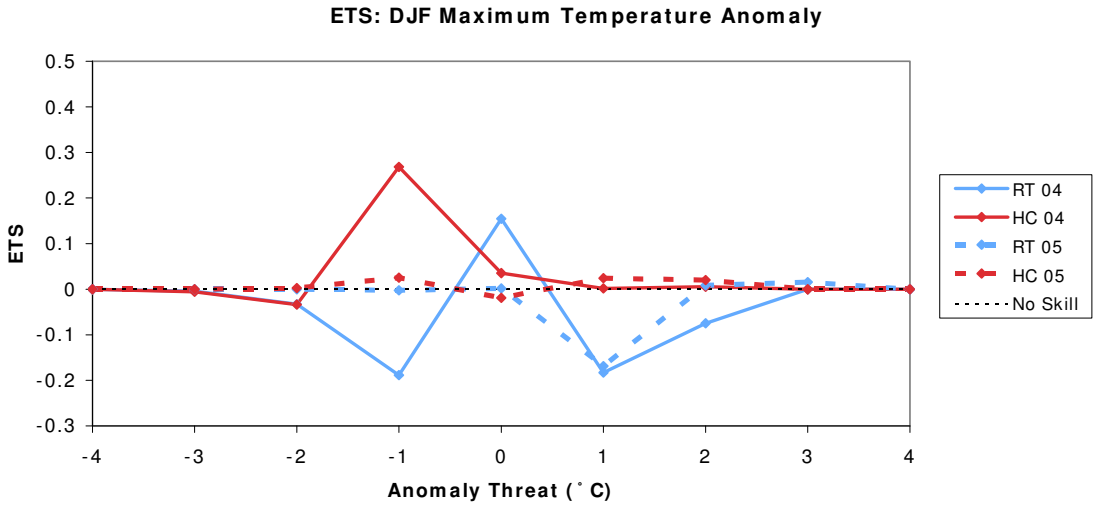

(a)

Figure 3.11. ETS for the seasonal (DJF) maximum (a) and minimum (b) forecasted temperature anomalies. Each figure plots scores from the 2004 real-time runs (solid blue), 2004 hindcast runs (solid red), 2005 real-time runs (dashed blue), 2005 hindcast runs (dashed red), and a line of no skill (dashed black).

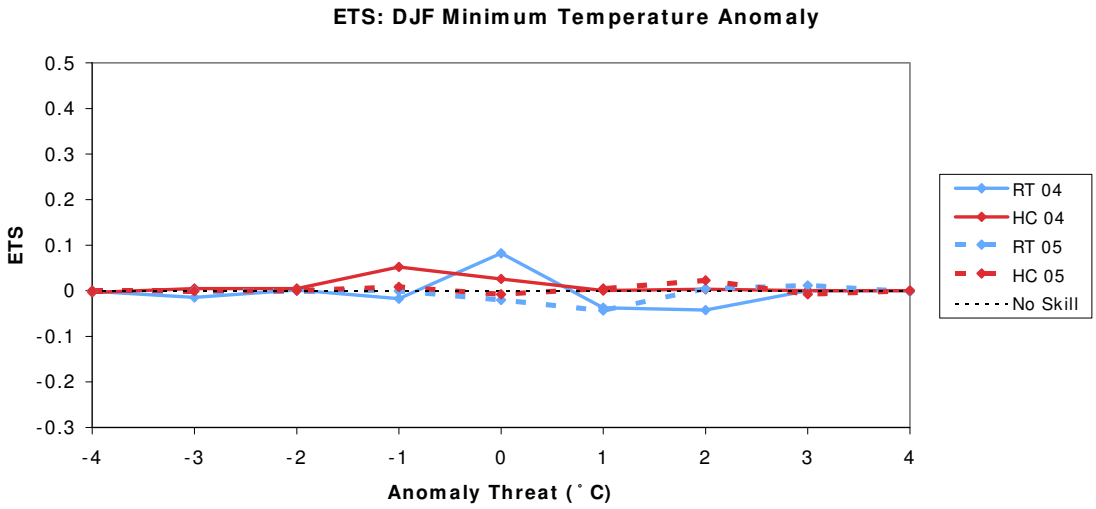

(b)

Figure 3.11 (Continued)

3.4 Extreme Events

Results in the previous sections show that the model has the capability to forecast monthly and especially seasonal maximum and minimum surface temperatures. Since the model is expected to be used as a tool to minimize losses and maximize profits in the agricultural community, additional evaluation of the model is needed. In the wintertime growing season of the southeast, unexpected anomalous frost and freeze events can lead to large amounts of agricultural damage. The type of crop, age of crop, or duration of the event all impact the exact amount of damage. In addition, the severity of the freeze or just how cold the temperatures drops and stay below freezing also influence the amount of dollars lost. Because of this, the model's ability to forecast daily frost and freeze events for four different thresholds is examined by counting the number of days the model outputs minimum temperatures below a freeze threshold during the winter season (DJF). Based on recommendations from the Florida Climate Center, 2°C, 0°C, -2°C, and -4°C thresholds are used (http://www.coaps.fsu.edu/climate_center/ website).

The real-time runs and hindcasts runs generally do an accurate job at capturing the pattern of frost/freeze events for the southeast in 2004 and 2005 (Figure 3.12) when examining minimum temperature forecasts. The models do particularly well in northern Florida and into

southern Alabama. For example, in 2004 both the real-time and hindcasts runs predict around 15-30 days below 0°C for this area, which is in agreement with the 15-30 days below 0°C that is observed. The real-time runs tend to under predict frost/freeze events in northern Alabama and Georgia, especially in the 2005 real-time runs when over 50 days of below 2°C minimum temperatures are observed, but the model only predicts between 25 and 40 days. Despite the real-time run's underestimation of freeze events in northern Alabama and Georgia, it does an excellent job at depicting how far south freeze events will occur in Florida, while the hindcast runs tend to over predict freeze events in south Florida. For these particular years, the hindcast runs show better skill at predicting the warmer thresholds or frost events (2°C and 0°C), while the real-time runs show more skill at predicting the coldest threshold (-4°C).

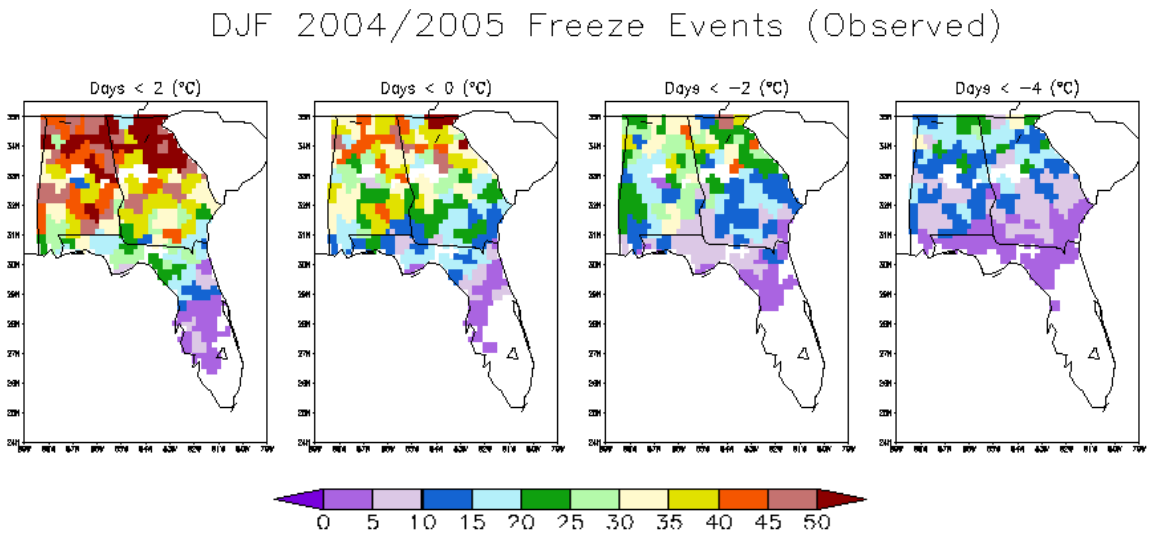

(a)

Figure 3.12. Daily counts frost and freeze events from the DJF 2004/2005 observations (a), real-time runs (b), and hindcast runs (c), as well as daily counts from the DJF 2005/2006 observations (d), real-time runs (e), and hindcast runs (f).

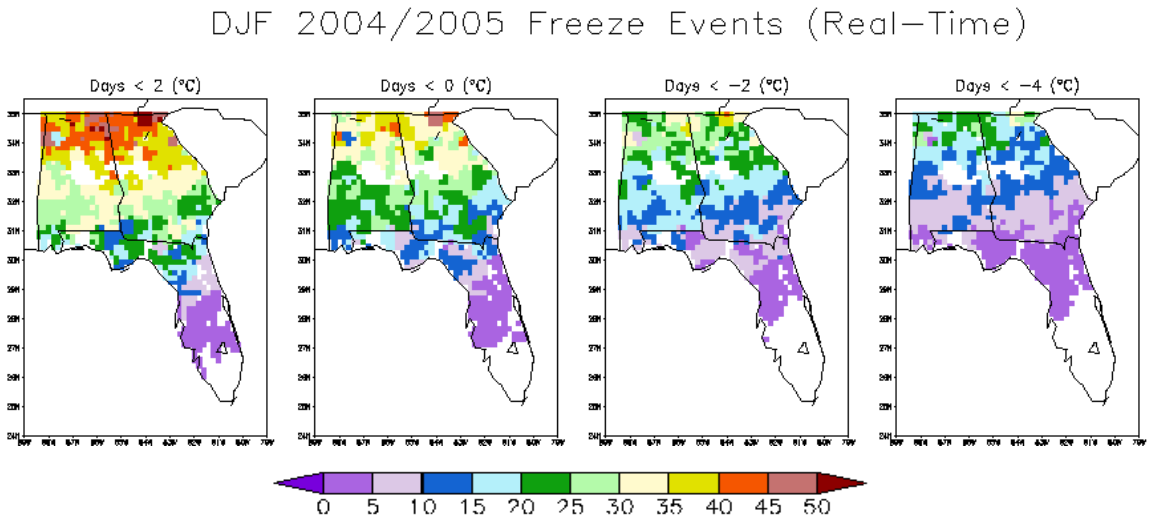

(b)

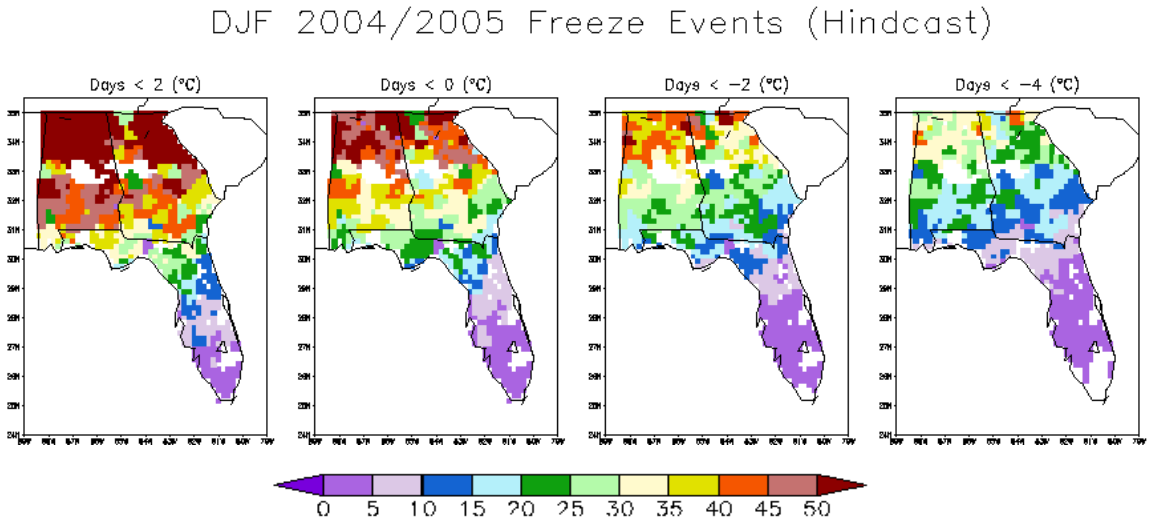

(c)

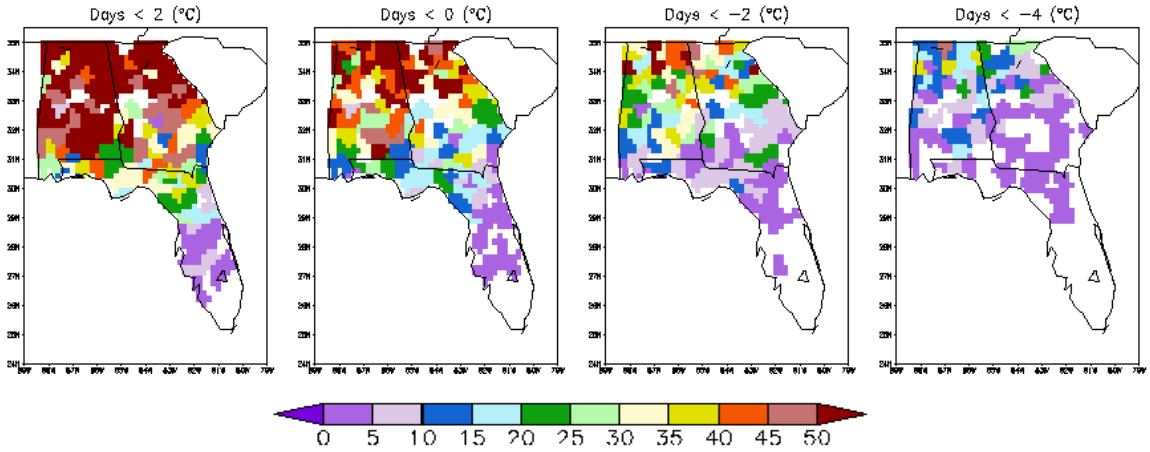

(d)

Figure 3.12 (Continued)

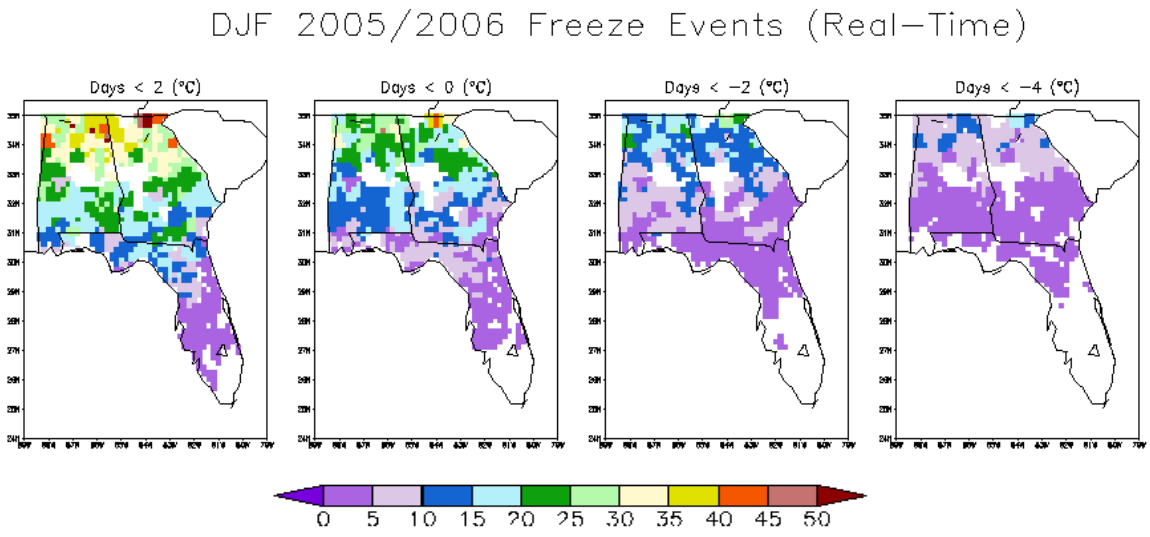

(e)

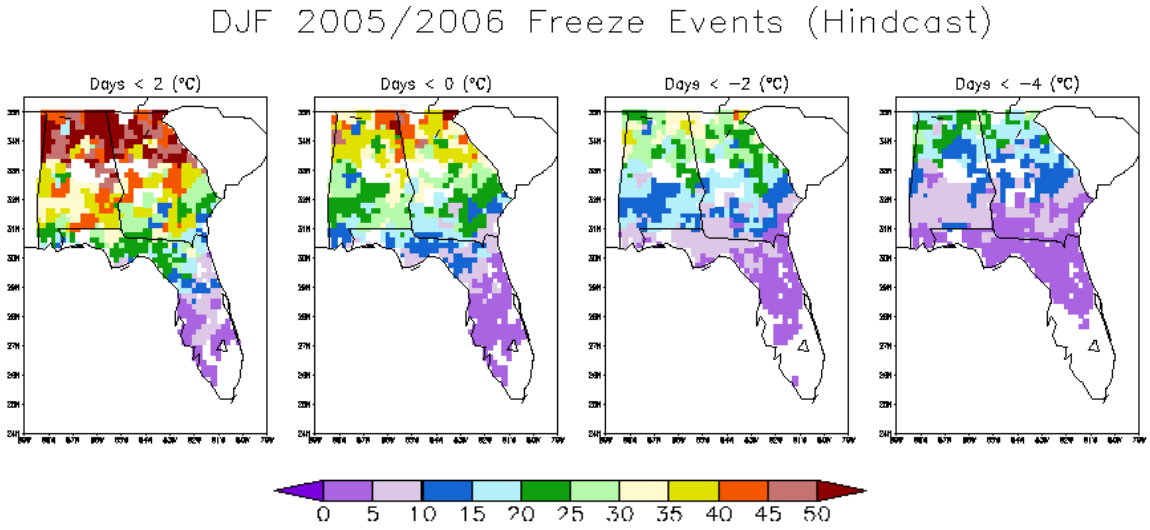

(f)

Figure 3.12 (Continued)

3.5 Discussion of Temperature Results and Tropical Pacific SSTA

As mentioned in Chapter 1, using persisted SSTA in climate models should produce forecasts comparable to those made from using prescribed SSTA if and only if the lower boundary conditions do not drastically change between the two forecasting methods during the forecasting time period. However, using a method of persistence can lead to large errors in the SST field and therefore errors in the model forecast if the anomalies take a sharp change during the forecast time period (Goddard and Mason, 2002). In 2004, using persisted SSTA leads to a

large area of positive SSTA errors over the tropical Pacific, but in 2005, the errors from using persisted SSTA are not as large and cover less of an area (Figure 1.1 a and b). Based on previous studies linking climate in the southeastern United States to tropical Pacific SSTs, the 2005 real-time and hindcast runs should produce similar forecasts, where as the 2004 real-time and hindcasts runs should differ in their predictions. More specifically, a loss of predictability is expected in the 2004 real-time runs due to the changes in SSTA over the tropical Pacific during the forecast period.

Despite the large positive SSTA errors that developed over the tropical Pacific in 2004 from using a method of persistence, the real-time and hindcast runs produce similar seasonal (DJF) maximum and minimum temperature forecasts in both 2004 (positive anomalies in south Florida and negative anomalies in northern Georgia and Alabama) and 2005 (positive anomalies across the entire southeast). This supports the idea of using prescribed SSTA for climate forecasting, but the 2004 real-time runs showing comparable predictability to the hindcast runs and in some areas, even outperforming the hindcast runs does not justify the need for coupled ocean-atmosphere models; however, results from previous studies (Montroy, 1996; Ropelewski and Halpert, 1986) indicate that the links between SSTA and temperature are more conclusive in southern Florida and the connection weakens the further north into Georgia and Alabama. Examining the 2004 seasonal forecasts more closely reveals that the hindcasts runs did outperform the real-time runs in southern Florida, where teleconnections are expected to be stronger. These previous studies combined with Taylor diagrams indicating the models show more predictability in 2005 (with correlation values closer to one and standard deviation values closer to what was observed) than in 2004, supports the theory that sharp changes in the tropical Pacific SSTA can lead to errors in model forecasts when using a method of persistence, and these results highlight the possible benefits of using a coupled model (assuming the changes in SSTA are correctly forecasted by the ocean model).

The effects of the SSTA error growth (caused from using persisted SSTA) during the October 2004 forecast period are not as evident when examining seasonal skill metrics or the daily counts of freeze events. The RMSE values, BS plots, ROC curves, and ETS indicate that the model performance varies between the 2004 and 2005 real-time and hindcast runs, showing little evidence of errors in SSTA playing a role in forecast skill. Also, the daily counts of freeze events in the wintertime (DJF) model forecasts suggests that the model's ability to capture freeze

events in the in the southeast is not greatly effected by using persisted SSTA in climate forecasting.

CHAPTER FOUR
RESULTS: PRECIPITATION FORECASTS

4.1 Ensemble Spread, Climatology, and Bias Correction

In addition to temperature, the real-time and hindcast December, January, and February precipitation forecasts are also evaluated due to their importance in crop modeling. Once again, averages of five ensemble members are used in validating precipitation forecasts. The ensemble spread for the daily precipitation model output does not start out initially small and then gradually increase with lead time (Figure 4.1), as seen in the temperature forecasts. From day one of the forecast, there are differences of over 27 mm between ensemble members. Throughout the forecast time period, the spread varies from day to day, indicating no long term (weekly, monthly, or seasonal) trends in the ensemble spread. The daily output time series of real-time and hindcast precipitation forecasts also reveals that the model consistently "precips out". In other words, the model unrealistically never predicts a daily precipitation amount of 0.0 mm. In addition to the model's inability to forecast the zero rainfall events, as expected, using the ensemble average (heavy dark line) leads to an underestimation of larger precipitation events. For example, in the October 2004 forecast, the largest magnitude in the ensemble average is close to 15 mm/day, but events of nearly 25 mm/day and even 30 mm/day are observed. To get a further perspective of the ensemble spread, the six (October through March) and three month (DJF) total precipitation for each ensemble member are calculated (Table 4.1). The individual totals indicate the sensitivity of the forecast to initial conditions in ensemble forecasting. With forecasting over 500 more millimeters of precipitation than any other ensemble member for the six month period, "ensemble 1" is clearly an outlier, and it overestimates the six month total precipitation by nearly 1000 mm. Despite this outlier, the other ensemble members still overestimate the observed six month precipitation by nearly 300 mm and the DJF total precipitation by roughly 200 mm. This overestimation of precipitation (wet bias), by almost twice the amount, is a noted problem with the FSU/COAPS regional model (Shin et al. 2005).

A comparison between the nineteen year monthly model climatology (from the hindcast runs) and observed monthly climatology confirms that the model has a wet bias in December, January, and February (Figure 4.2). For all three months, the model tends to have a 1-5 mm/day wet bias over the majority of Florida and throughout the southeast coast of Georgia. The bias is strongest along the eastern coast of Florida, especially in December. This wet bias along the eastern coast of Florida is probably due to the model's already noted cold bias air coming in contact with the warmer Gulf Stream. The model also has a dry bias between -1 mm/day and up to -4 mm/day in western Alabama for these three months. The dry bias is most significant in the southeast corner of Alabama in January. As discussed in the previous chapter, all models have systematic errors, and to account for the FSU/COAPS NRSM systematic errors, bias correction is performed on the precipitation data.

A variety of techniques can be used to bias correct model precipitation data, and the best method is still being debated today. For this study, a technique similar to the temperature bias correction is used:

$$P_{bc} = (P_m / \overline{P}_m) \times \overline{P}_o$$

where P_m is the daily model forecasted precipitation, $\overline{P}_m$ is the 19 year model monthly climatology, and $\overline{P}_o$ is the 19 year observed monthly climatology . In an attempt to account for the model consistently precipitating out (Figure 4.1), any daily precipitation less than a trace (0.254 mm) is set to zero. After bias correction, the model shows the greatest improvement for the first 30 days of the forecast (Figures 4.3 and 4.4). This is most likely due to the fact that the October model climatology has a strong wet bias across the entire southeast (Figure 4.5). After 30 days, the improvement of the precipitation bias correction is slight, which is probably an effect of only plotting the area averaged bias corrected precipitation. As discussed previously, the model has a wet bias along the eastern coast of Florida and then a dry bias in western Alabama. These biases are in a sense canceling each other out when plotting the area average. A spatial plot comparing the errors in six month average precipitation forecasts from the 2004 real-time model runs before and after bias correction reveals that bias correcting reduces systematic errors in the majority of Florida and Georgia, but actually created a wet bias in western Alabama (Figure 4.6). As with the temperature results, bias corrected data is used to

examine the model's ability to forecast precipitation, except when validating anomalies or the percent from normal precipitation.

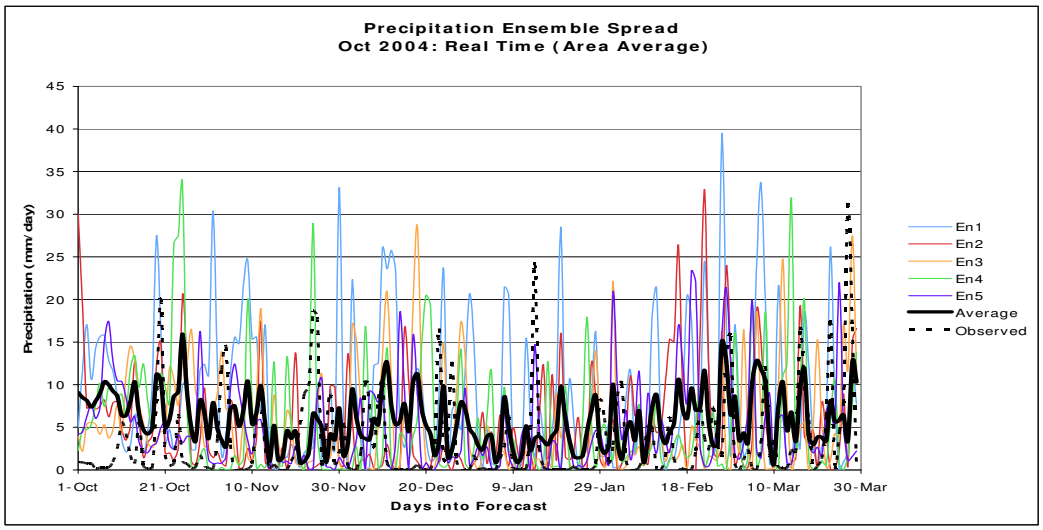

Figure 4.1. Daily precipitation model output and observations from the October 2004 real-time runs area averaged over Florida, Georgia, and Alabama. The chart displays output for all five individual ensemble members (blue, red, orange, green, and purple), the ensemble average (black bold), and what was observed (black dashed).

Table 4.1. Six month (October through March) and three month (December through February) accumulation of precipitation from the five October 2004 real-time ensemble members, the ensemble average, and observations.

	Total Precipitation (mm) Oct 2004: Real Time	
	6 Months	DJF
Observed	602.6	236.8
En1	1558.0	788.4
En2	895.8	417.0
En3	977.2	399.1
En4	947.3	345.0
En5	900.1	443.0
Average	1055.7	478.5

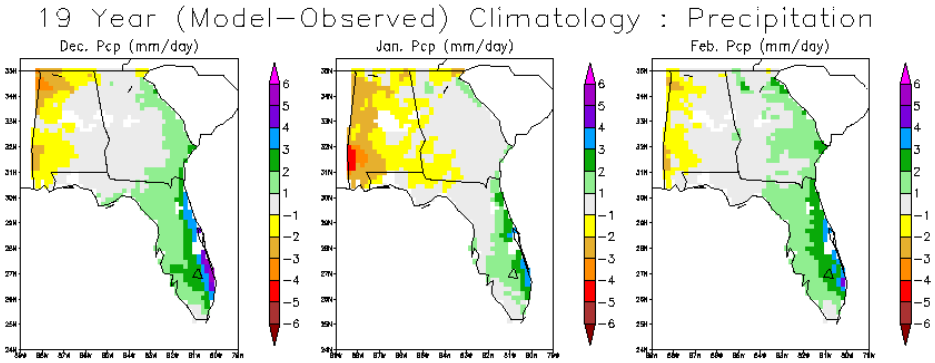

Figure 4.2. The difference between the nineteen year monthly model precipitation climatology and the 19 year monthly observed precipitation climatology in December (left), January (center), and February (right). The model climatology originates from nineteen years of October hindcasts runs.

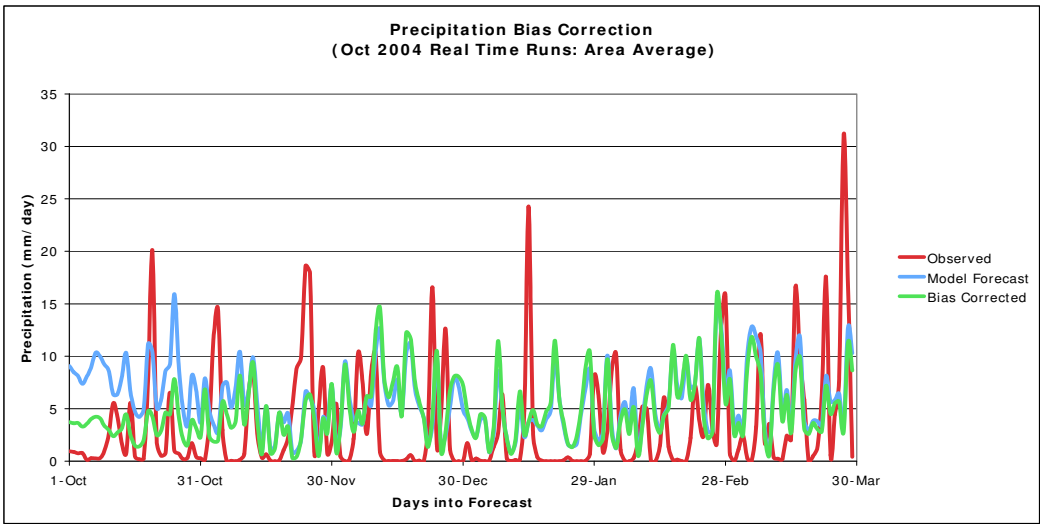

Figure 4.3. Daily precipitation output from the October 2004 real-time model runs (blue), the October 2004 bias corrected real-time runs (green), and what was observed (red) area averaged over Georgia, Alabama, and Florida.

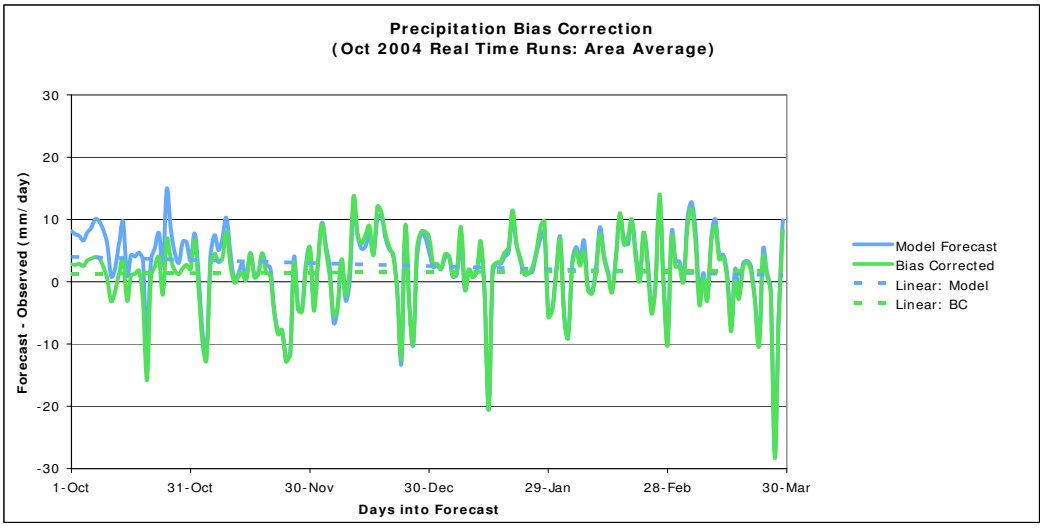

Figure 4.4. Area averaged (over Georgia, Alabama, and Florida) daily forecasted precipitation minus the area averaged observed precipitation from the October 2004 real-time run (solid blue) and October 2004 bias corrected real-time run (solid green). A line of linear fit is also plotted for both the raw forecast (dashed blue) and bias corrected forecast (dashed green).

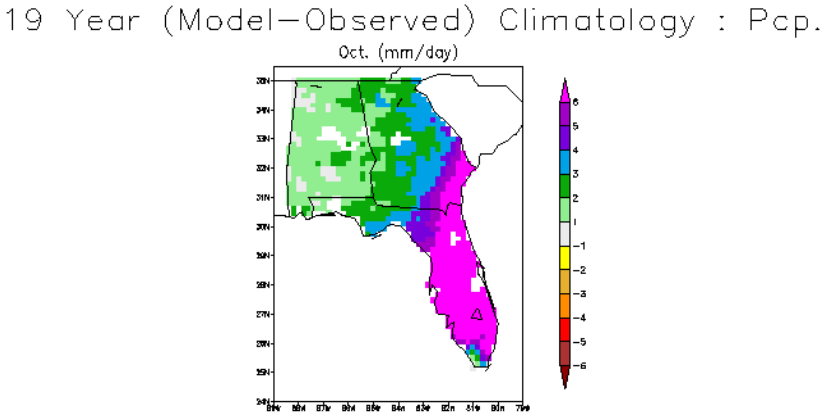

Figure 4.5. The difference between the nineteen year October model precipitation climatology and the nineteen year October observed precipitation climatology. The model climatology originates from nineteen years of October hindcasts runs.

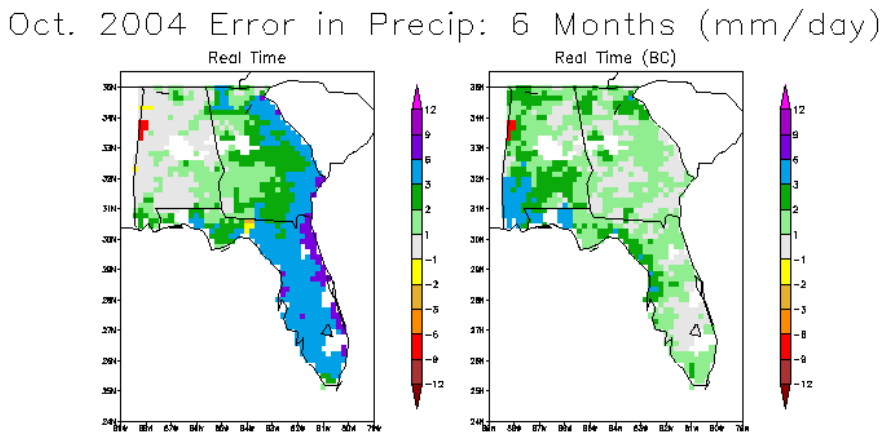

Figure 4.6. The six month (October through March) error in precipitation (mm/day) from the October 2004 real-time model runs before bias correction (left) and after bias correction (right).

4.2 Seasonal/Monthly Predictions

An important goal of climate modeling is the ability to predict the departure from normal precipitation. For this study, the model's seasonal and monthly percent from normal precipitation is determined by:

$$\%\ \text{from normal} = (P_m / \overline{P}_m) \times 100\%$$

where P_m is the forecasted(observed) precipitation (mm/day) and $\overline{P}_m$ is the nineteen year model(observed) climatology (mm/day). For example, to calculate the model's forecasted departure from normal precipitation for a given month, P_m would be the model forecasted daily precipitation averaged over a thirty day period, and $\overline{P}_m$ would be the monthly model climatology. Again, the hindcast model climatology is used for both bias correction of hindcast and real-time runs. Using the hindcast climatology to bias correct the real-time runs could possibly lead to an underestimation of real-time skill and should be considered when evaluating results.

The DJF seasonal precipitation forecasts from both the October 2004 and 2005 real-time and hindcast runs are examined. Observations indicate the southeast ended with below average rainfall for the 2004/2005 winter season with the majority of the percent from normal ranging between 50-80 % (Figure 4.7a). The 2004/2005 winter real-time runs incorrectly forecast above

normal precipitation for the southeast, resulting in large errors (some greater than 100%) across the southeast. The 2004/2005 winter hindcast runs are more accurate at predicting the seasonal percent from normal than the 2004 real-time runs. The hindcast runs correctly forecast below average precipitation for most of the southeast; however, the model under predicts just how dry it will be and it leads to some 10-35% errors. For the 2005/2006 winter season, the southeast is again predominantly drier than average, but with only areas over southern Florida reporting less than 50% of normal precipitation it is not as dry as the 2004/2005 season (Figure 4.7b). Also, a band of above normal precipitation across the Florida/Georgia border occurs in the 2005/2006 winter season. The 2005/2006 winter real-time and hindcast seasonal precipitation forecast look almost identical. Both models correctly predict slightly drier than normal precipitation for the majority of the southeast, but the models do not capture the band of above normal precipitation observed across northern Florida and southern Georgia, resulting in greater than 35% errors.

Taylor diagrams are also created for the seasonal precipitation forecast to easily compare model statistics. In 2004, the hindcast runs provide a forecast closer to what was observed than the October 2004 real-time runs in terms of correlation, standard deviation, and RMS values (Figure 4.8). The 2004 hindcast runs have a similar result to a forecast of climatology, with the exception of climatology having a correlation value closer to one. With a correlation less than 0.55 and a normalized standardized deviation of 1.2, the October 2004 real-time runs are not able to capture the observed precipitation pattern in comparison the hindcast runs. In 2005, the real-time runs, hindcast runs, and climatology all have similar statistics. Again, as in the 2004/2005 winter season, climatology has the forecast closest to what was observed.

The monthly precipitation forecasts for December, January, and February 2004/2005 and 2005/2006 winter season are also evaluated. As expected from the seasonal forecasts, the 2004 real-time runs over predict monthly rainfall throughout the southeast (Figure 4.9a). Forecast errors in the departure from normal precipitation of over 100% occur in all three months. In December, precipitation forecasts over Alabama and Georgia result in the largest errors, where as in January, the largest errors occur along the Gulf coast. In February, the 2004 real-time runs still over predict rainfall in southern Alabama, but errors in Georgia and northern Florida are less extreme and stay between -35% and 35%. The 2004 January hindcast runs are similar to the real-time runs in over predicting the amount of precipitation, but the hindcast runs do not have the same strong wet bias along Florida's Gulf coast. The 2004/2005 December and February

hindcast runs differ than the real-time runs and tend to under predict precipitation. The majority of errors from the 2004 hindcast runs stay between -50 to 50%. The 2005/2006 real-time and hindcast runs produce very similar monthly departure from normal precipitation forecasts (Figure 4.9b). Both 2005 model runs under estimate precipitation in December and February, especially along the Florida/Georgia border which results in greater than 50% errors. In all three months from the October 2005 model runs, the real-time runs tend to produce slightly drier precipitation forecasts than the hindcast runs.

Taylor diagrams for the monthly precipitation forecasts from the October 2004 and 2005 model runs are created. Considering the standard deviation, correlation, and RMS values, the 2004 real-time runs struggle in forecasting the monthly precipitation for the southeast in December, January, and February (Figure 4.10); however, both the 2004 hindcast runs as well as a forecast of climatology stray from the reference point and like the real-time runs, appear to have difficulties in predicting the January 2005 precipitation. The 2004 hindcast runs and climatology are similar for all three months and consistently outperform the real-time runs in correlations, standard deviations, and RMS values. In 2005 the real-time runs, hindcasts runs, and climatology results are clustered together for all three months, and indicate no pattern of one particular forecast method outperforming the other.

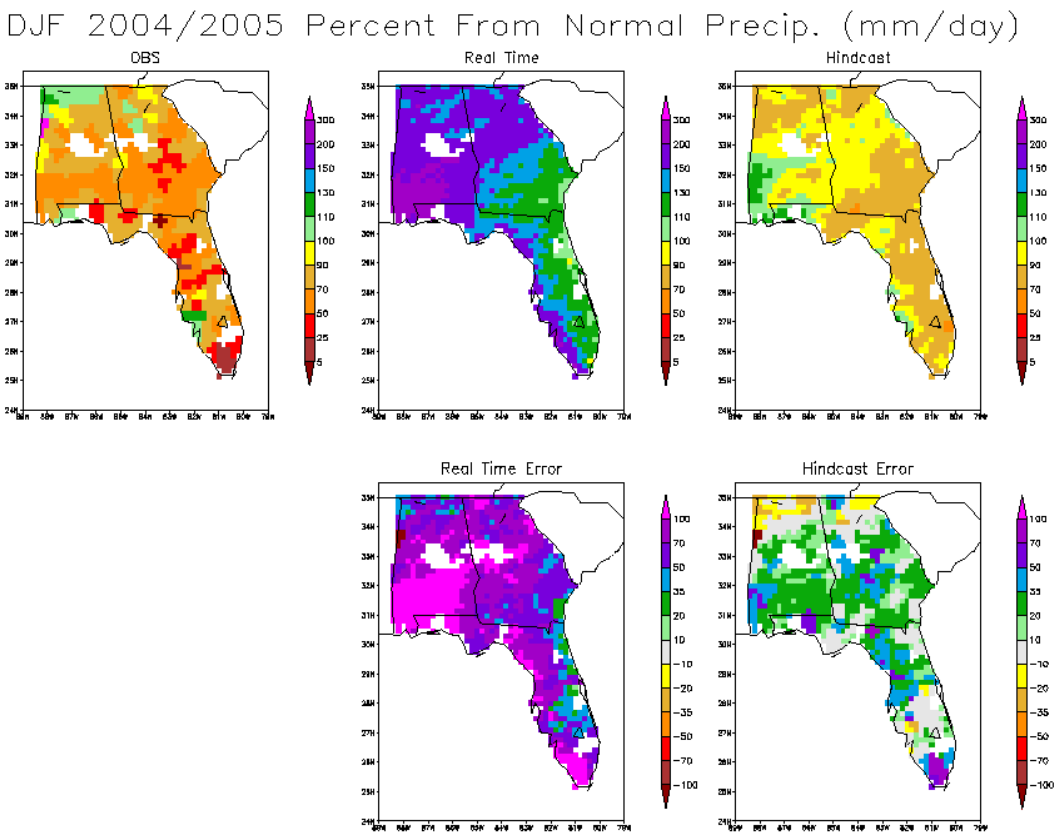

(a)

Figure 4.7. Spatial plots of the DJF 2004/2005 precipitation (a) and DJF 2005/2006 precipitation (b) model forecasts (2 month lead time). Each group of figures plot the observed departure from normal precipitation (top left), the forecasted real-time departure from normal precipitation (top center), the forecasted hindcast run anomaly (top right), the difference between the observed anomaly and the real-time forecasted anomaly (bottom center) and the difference between the observed anomaly and the hindcast forecasted anomaly.

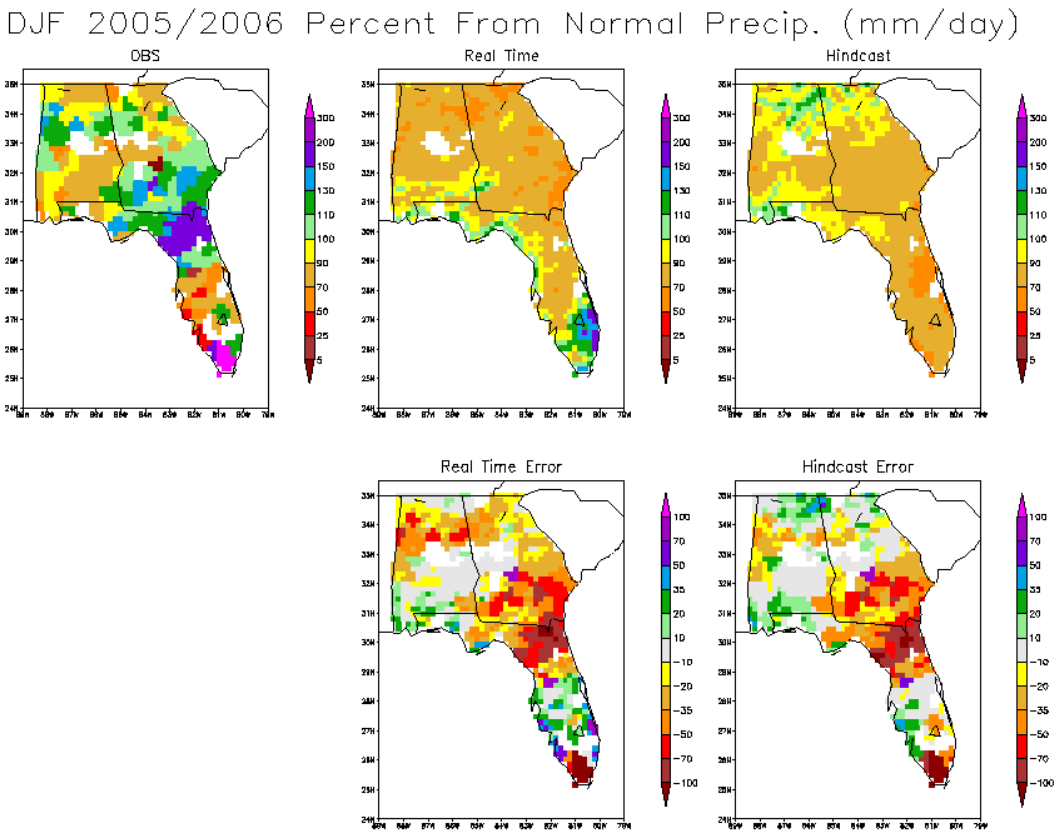

(b)

Figure 4.7 (Continued)

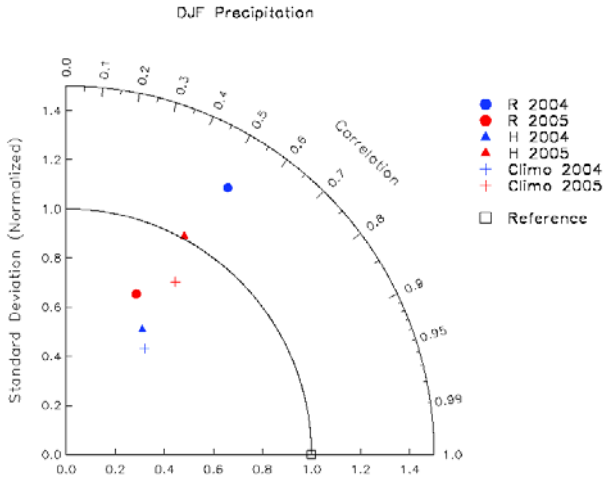

Figure 4.8. Taylor diagram of the DJF precipitation forecasts. The plots include results from the 2004 real-time runs (blue circles), 2005 real-time runs (red circles), 2004 hindcast runs (blue triangles), 2005 hindcast runs (red triangles), 2004 climatology forecast (blue crosses), 2005 climatology forecast (red crosses), and a perfect forecast reference point (black squares).

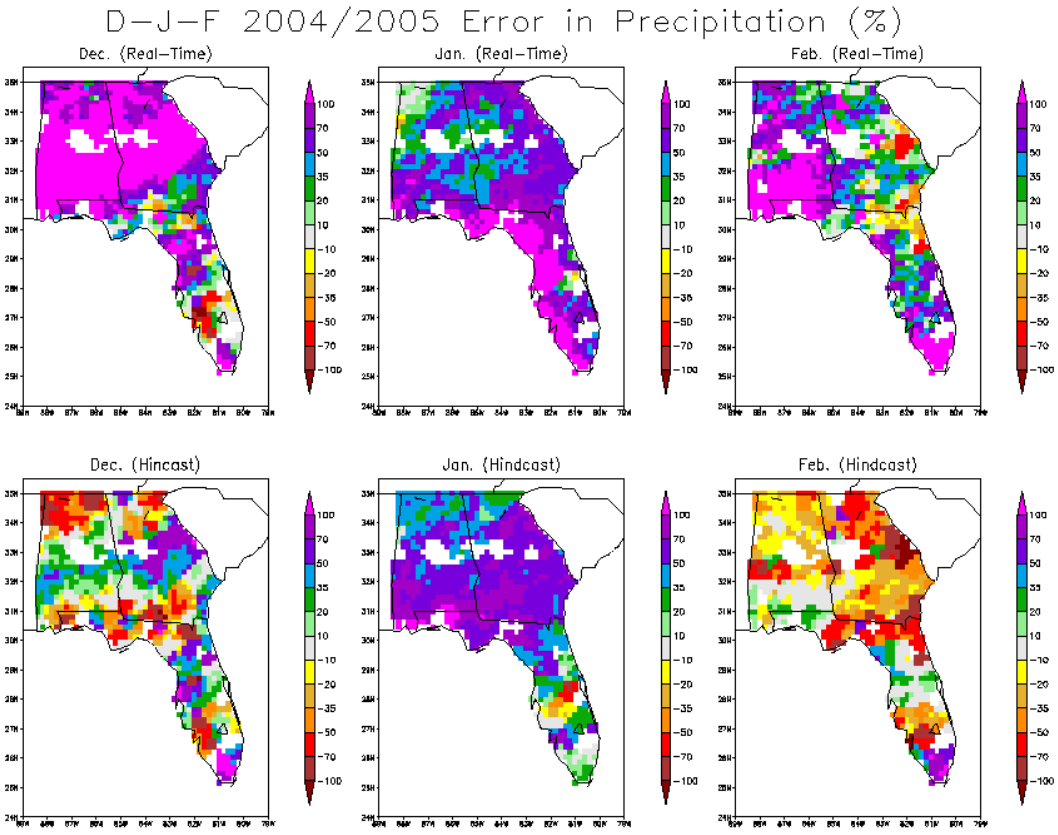

(a)

Figure 4.9. The model forecasted minus the observed monthly departure from normal precipitation (model error) for December, January, and February (2, 3, and 4 month lead times) 2004/2005 model runs (a) and 2005/2006 model runs. Each figure has error results from the real-time runs (top row) and hindcast runs (bottom row) monthly anomaly forecasts from December (left), January (center), and February (right).

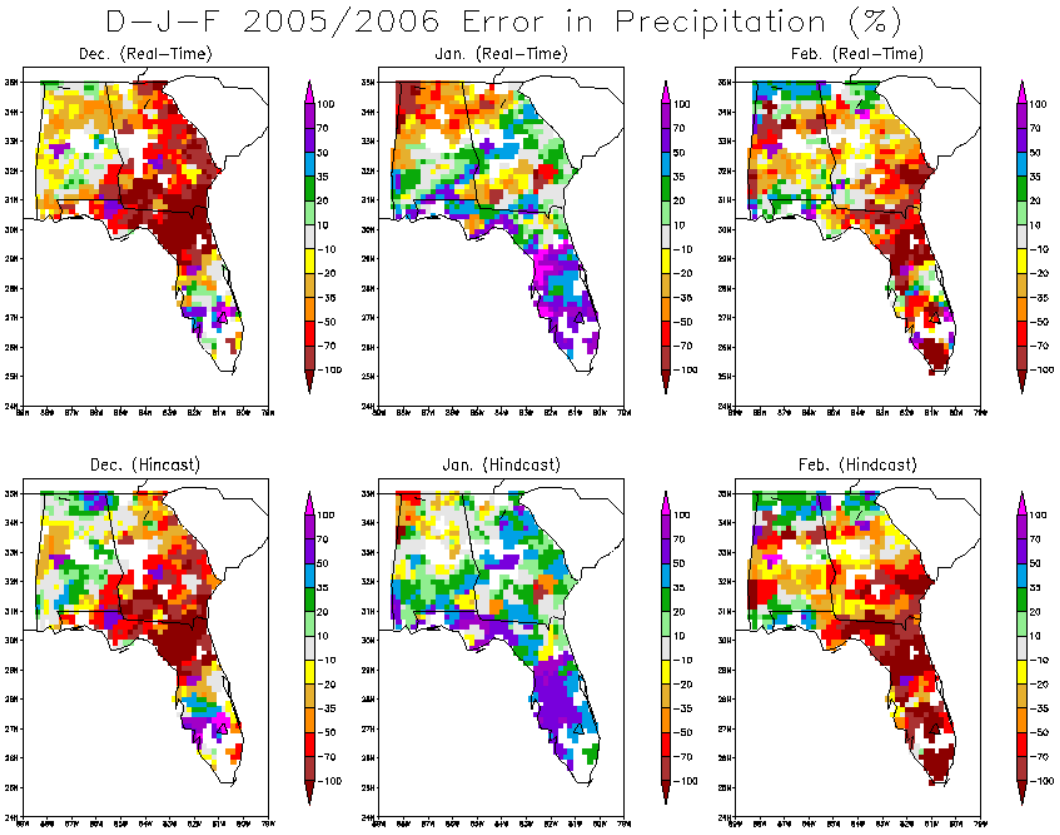

(b)

Figure 4.9 (Continued)

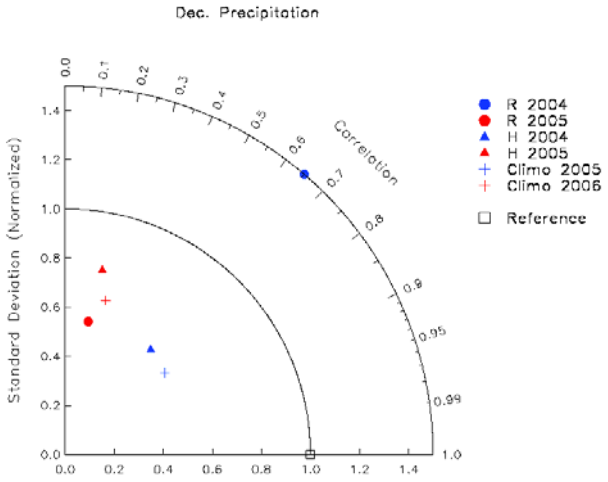

(a)

Figure 4.10. Taylor diagrams from the December (a), January (b), and February (c) precipitation forecasts. The plots include results from the 2004 real-time runs (blue circles), 2005 real-time runs (red circles), 2004 hindcast runs (blue triangles), 2005 hindcast runs (red triangles), 2004 climatology forecast (blue crosses), 2005 climatology forecast (red crosses), and a perfect forecast reference point (black squares).

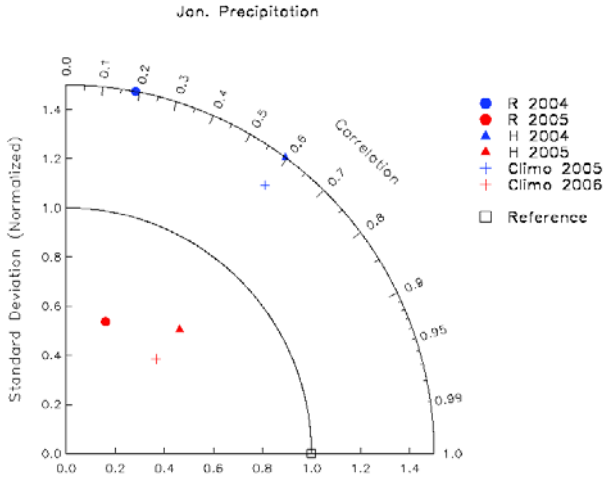

(b)

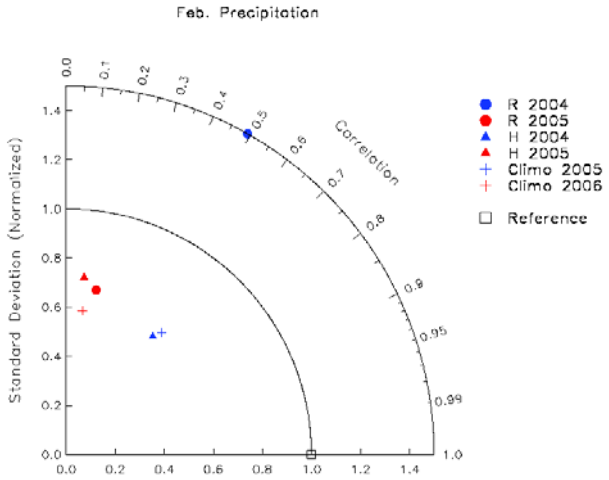

(c)

Figure 4.10 (Continued)

4.3 Skill Scores and Standard Verification Methods

The same skill scores and other standard verification methods that were used to determine the value of temperature forecasts are also used to evaluate precipitation forecasts. This includes the RMSE values, BS, ROC curves, and ETS. The 2004 real-time runs stand out as showing little skill when compared to the 2005 real-times runs and well as the 2004 and 2005 hindcast runs. For example, with an RMSE of 94.78%, it nearly doubles the values from the 2005 model runs (Table 4.2). The BS shows the 2004 real-time runs fall below both the

reference forecasted (created from nineteen years of observed data) and the hindcast runs for all thresholds, but has particular trouble at forecasting a -1 mm/day anomaly (Figure 4.11). ROC curves (Figure 4.12) and ETS (Figure 4.13) plots also indicate the 2004 real-time runs' lack of skill in predicting precipitation; however, the 2004 hindcast runs show potential with BS scores close to the reference forecast and ROC curves above the line of no skill for positive and negative 5 mm/day thresholds. The 2004 hindcast runs do particularly well at forecasting a positive 5 mm/day anomaly. Following suit with seasonal and monthly results, the 2005 real-time and hindcasts runs produce similar skill scores with RMSE values within 2% of each other. Both the 2005 real-time and hindcast runs result in a BS similar to the reference forecast, with the hindcast runs showing slightly better results than the real-time runs for a neutral anomaly. The ROC curves also indicate that the 2005 hindcast runs are able to predict a neutral threshold better than the 2005 real-time runs, but the ROC curves show that the real-time runs do better at predicting a -5 mm/day anomaly.

Table 4.2. RMSE values for the seasonal (DJF) departure from normal precipitation forecasts from the October 2004 and 2005 model runs.

RMSE: DJF Departure From Normal Precipitation (%)		
	2004	**2005**
Real-Time	95	57
Hindcast	45	59

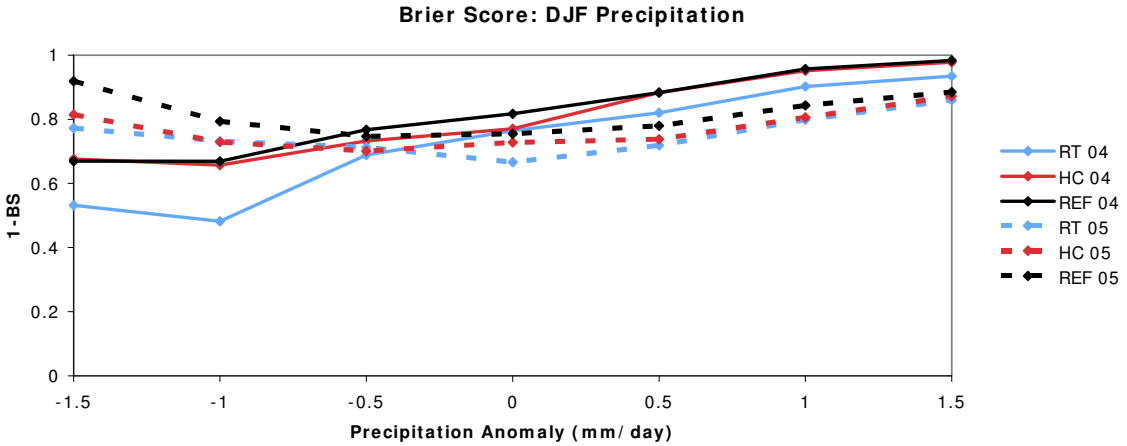

Figure 4.11. BS for the seasonal (DJF) forecasted precipitation anomalies. The figure plots scores from the 2004 real-time run (solid blue), 2004 hindcast run (solid red), a 2004 reference forecast (solid black), 2005 real-time run (dashed blue), 2005 hindcast run (dashed red), and a 2005 reference forecast (dashed black).

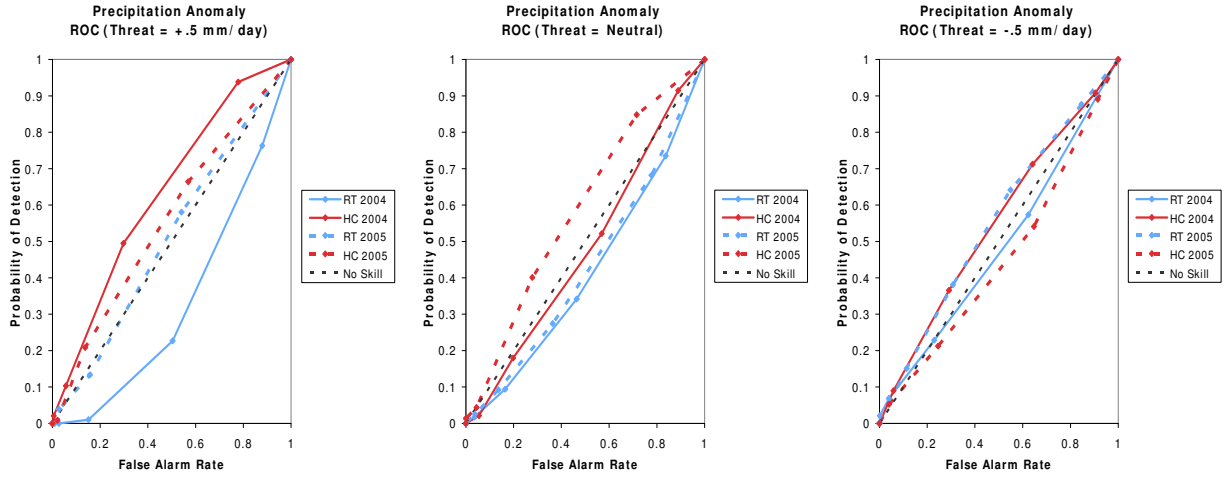

(a) (b) (c)

Figure 4.12. ROC curves for precipitation anomalies for a positive 0.5 mm/day (a), neutral (b), and negative 0.5 mm/day (c) threshold. Each figure plots curves representing the 2004 real-time runs (solid blue), 2004 hindcast runs (solid red), 2005 real-time runs (dashed blue), 2005 hindcast runs (dashed red), and a line of no skill (dashed black).

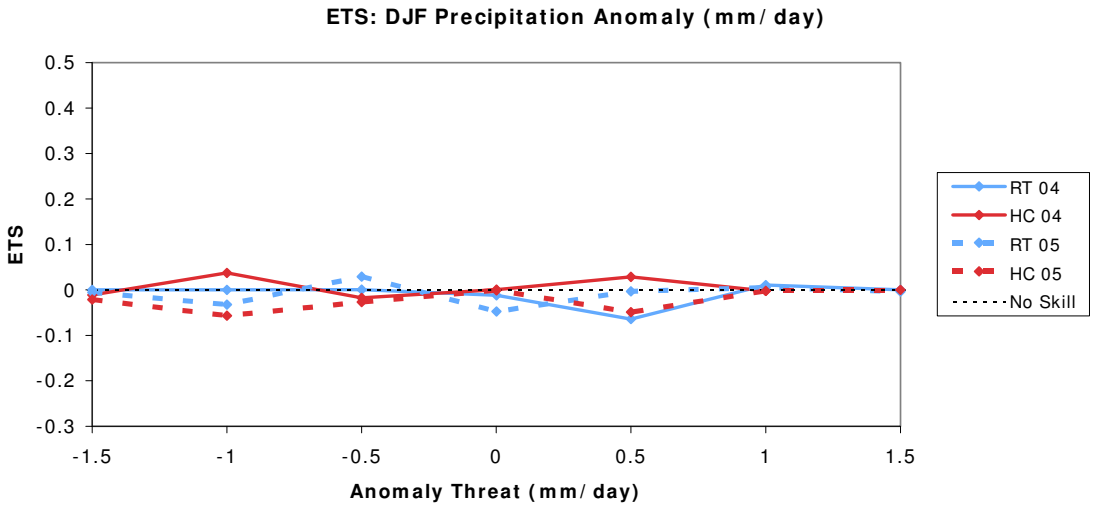

Figure 4.13. ETS for seasonal (DJF) precipitation anomalies. The figure plots scores from the 2004 real-time run (solid blue), 2004 hindcast run (solid red), 2005 real-time run (dashed blue), 2005 hindcast run (dashed red), and a line of no skill (dashed black).

4.4 Extreme and Daily Precipitation Events

If the FSU/COAPS climate model real-time runs are to be used in crop models to benefit the southeast's agricultural community, then the ability to forecast seasonal and monthly anomalies should not be the only concern. Just as winter freeze events (discussed in the previous chapter) can impact crops, so can anomalously large precipitation events. In this study, greater than 12 mm/day (0.5 inches/day) of precipitation was considered a "heavy precipitation" event. Although 12mm does not seem like a threatening precipitation event, receiving multiple days of above 12mm of precipitation in one season (especially during south and central Florida's dry season) can cause an abundance of damage to crops. The real-time and hindcast model runs from both 2004 and 2005 capture the general pattern of heavy precipitation events in the southeast (a higher frequency of events occurring in Alabama and northern Georgia and few events occurring throughout Florida) (Figure 4.14). In 2004, the real-time runs over estimate the number of heavy rainfall events and especially struggle in northern Alabama and Georgia where over 12 days of greater than 12 mm of precipitation are forecasted, but mostly only 8-10 days of heavy precipitation are observed. The hindcast runs are more accurate at predicting the number of heavy precipitation events than the real-time runs in 2004; however, the hindcast runs under estimate the number of days with greater than 12 mm of precipitation in northern Alabama and

Georgia. Similar to the 2004 real-time forecast, the 2004 hindcast runs also over estimate the number of heavy precipitation days in Florida. In 2005, the real-time and hindcasts runs result in similar predictions of heavy precipitation events. Both forecasts resemble what was observed, with the exception of the models being slightly too dry in most of Georgia and Alabama. Also, the real-time runs are more accurate than the hindcast runs at capturing the greater number of heavy precipitation events that occurred in Alabama during the 2005/2006 winter season.

In an attempt to get an even better idea of how the models predict other amounts of daily rainfall, counts for various precipitation thresholds are created. In 2004, both the models indicate a wet bias in predicting the number days of greater than 5 mm of precipitation (Figure 4.15a). The 2004 real-time runs continue to over predict daily rainfall with increasing thresholds. The 2004 hindcast runs are comparable to observations at a threshold of 10 mm/day, begin to under estimate daily rainfall events for thresholds greater than 15 mm/day, and then the hindcast runs prediction of daily rainfall events again resembles observations for thresholds greater than 35 mm/day. The counts of daily precipitation events look similar for both the real-time and hindcasts run from 2005 (Figure 4.15b). Both models tend to under predict daily rainfall for all thresholds, but the real-time run counts are slightly closer to what was observed. With the exception of the 2004 real-time runs, the models appear very capable of capturing the higher rainfall amounts (greater than 35 mm/day).

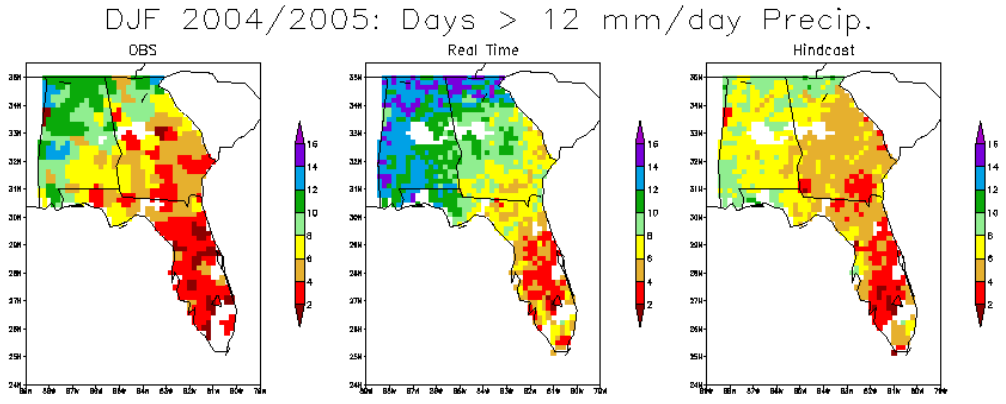

(a)

Figure 4.14. Daily counts of heavy precipitation events from the DJF 2004/2005 (a) observations (left), real-time runs (center), and hindcast runs (right), as well as daily counts from the DJF 2005/2006 (b) observations (left), real-time runs (center), and hindcast runs (right).

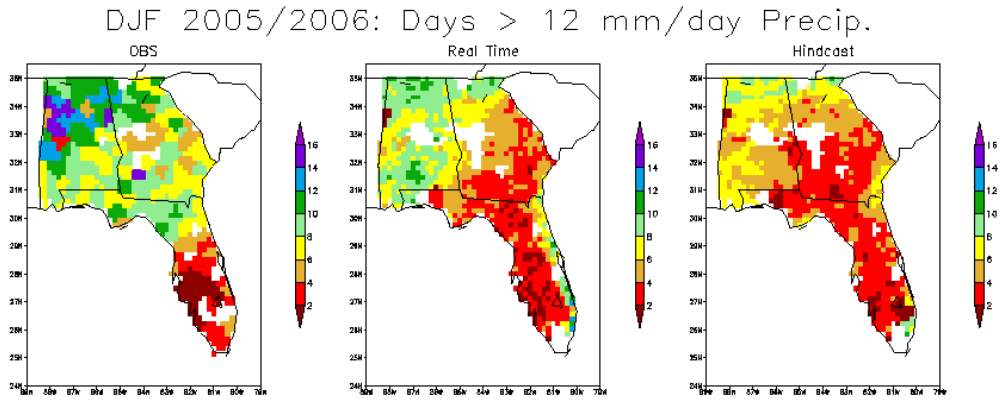

(b)

Figure 4.14 (Continued)

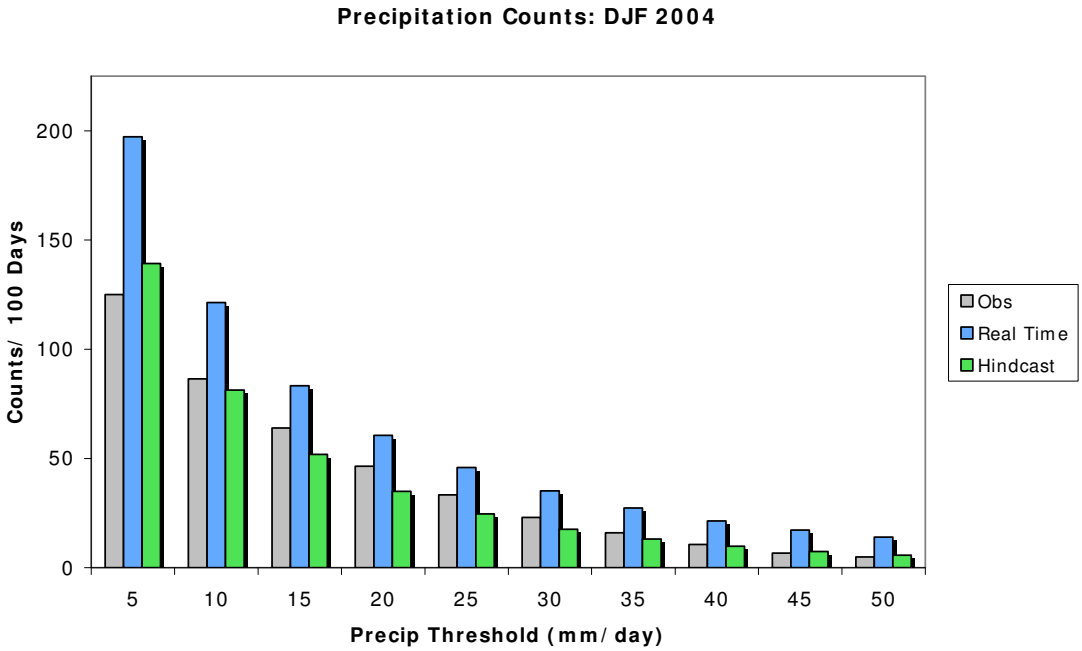

(a)

Figure 4.15. Daily counts of observed (gray), real-time (blue), and hindcast (green) precipitation events for various thresholds from the DJF 2004/2005 (a) and DJF 2005/2006 (b) seasons.

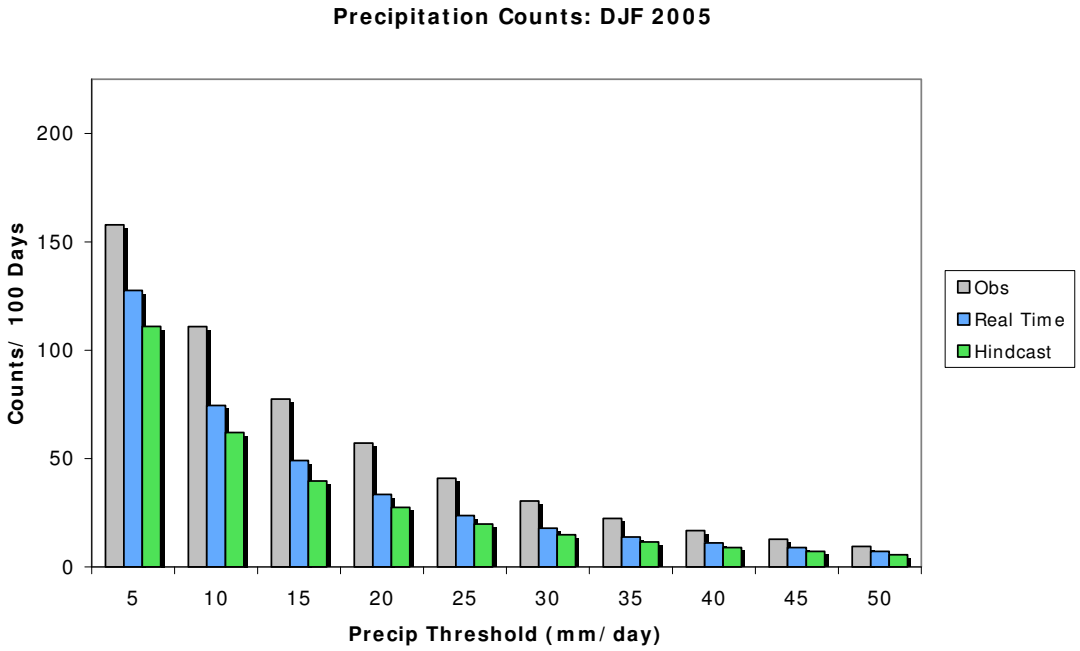

(b)

Figure 4.15 (Continued)

4.5 Discussion of Precipitation Results and Relation to Tropical Pacific SSTA

Although only using two years of model runs, the disadvantages of using persisted SSTA to predict seasonal and monthly precipitation in the southeastern United States seem obvious. In 2004, when the large positive errors in the tropical Pacific SSTA develop early in the forecast period (Figure 1.1a), the hindcast runs (which use updated weekly prescribed SSTs) consistently outperform the real-time runs (which use persisted SSTA) in both seasonal and monthly forecasting. In 2005, the SSTA in the tropical Pacific remain fairly constant throughout the first weeks of the forecast period (Figure 1.1b). Not only do the 2005 real-time runs significantly improve (in comparison to the 2004 real-time runs), but the monthly and seasonal precipitation forecasts are remarkably similar between the 2005 real-time and hindcast runs. Evaluating skill scores and other skill metrics also indicate that using a method of persistence in climate forecasting leads to a loss of precipitation predictability in the southeast when equatorial Pacific SSTA do not remain fairly constant during the forecast period. RMSE values, BS, ROC curves, and ETS all show that the 2004 real-time runs result in the least amount of skill in comparison to the 2005 real-time runs and both years of hindcast runs. Finally, although the model is able to

capture the general pattern of heavy precipitation during the winter season (DJF) in both 2004 and 2005 forecasts, the 2004 real-time runs overestimate daily precipitation events for all thresholds. The same strong wet bias does not occur in the 2004 hindcast runs, suggesting that the SSTA error growth over the tropical Pacific (caused from using persisted SSTA) in the 2004 real-time runs led to a loss of predictability.

CHAPTER 5
SUMMARY, CONCLUSIONS, AND FUTURE WORK

A growing understanding of the atmosphere and its' links to tropical SSTs combined with an increased number of climate models and length of forecast time periods has led to a rising need for climate model verification and strategies for conducting climate model studies. This study specifically examined the FSU/COAPS NRSM and its' ability to forecast seasonal wintertime (2 month lead time) surface temperature and precipitation over the southeastern United States. The real-time model's output was also compared to model runs made using weekly updated observed SST in an attempt to examine the disadvantages of using persisted SSTA in climate forecasting. The potential of using the FSU/COAPS real-time runs in crop models to minimize losses and maximize profits in the southeastern United States' agricultural community motivated this study. Conclusions on the models predictability, the possible benefits of a coupled model, and the current problem areas of the model's physics can be made from this study.

The 2004 and 2005 wintertime real-time model forecasts showed potential of predictability in forecasting wintertime surface temperatures and precipitation over the southeastern United States. The model was particularly capable of forecasting the seasonal maximum and minimum temperatures with the majority of anomaly errors below 3°C, correlations close to one, small RMS values, and standard deviations similar to observations (Figures 3.5 and 3.6). Despite showing reasonable skill in seasonal temperature forecasts, the model was inconsistent in seasonal precipitation forecasts. In 2005, the model showed little error in departure from normal precipitation, but then in the 2004 runs, the model overestimates precipitation in the southeast by over 150% (Figure 4.5). Taylor diagrams also indicated that the model had difficulty in producing precipitation fields similar to what was observed (Figure 4.6). Both the temperature and precipitation model predictability appeared to break down when analyzed on a monthly time scales, with errors in anomalies and departures from normal varying greatly from month to month (Figures 3.7, 3.8, 4.7, and 4.8). However, results indicated that the

model had the capability to predict the number of daily freeze events and heavy precipitation events for the winter time season (Figure 3.12, 4.12, and 4.13). This demonstrates that intraseasonal variability is still very difficult to achieve. The ability to forecast the number of these agriculturally threatening anomalous events could potentially be of value to farmers. Climate prediction still remains to be a challenging task, especially when equatorial SSTA are at a minimum in magnitude. Neither of years examined (2004 or 2005) were strong ENSO events, and as expected, when comparing the model forecast to a forecast of climatology or when evaluating skill scores, the model appears to show a lack of predictability of temperature and precipitation over the southeast. However, model forecasts falling only slightly behind a forecast of climatology when SSTA in the tropical Pacific remain fairly constant suggest that there is potential in climate modeling. In order to truly evaluate the model's forecasting capabilities, years with large SSTA should be evaluated.

Comparing real-time runs to hindcast runs highlighted the drawbacks of using persisted SSTA for climate modeling. The precipitation results were more conclusive than temperature, with much greater errors and a clear loss of skill when equatorial Pacific SSTA took a sharp change within weeks of the 2004 forecast period. The fact that the model real-time and hindcasts runs were so similar in the October 2005 DJF precipitation forecasts (when tropical Pacific SSTA remained fairly constant) indicated that teleconnections exist between tropical SSTA and climate in the southeast exits in the model. Although, no hindcast runs to compare it to, the October 2006 real-time run preliminary results supports the theory that using prescribed SSTA in climate models will lead to a loss of predictability (Figure 5.1) if SSTA in the tropical Pacific take a sharp change early in the forecast period (Figure 5.2), as they did in the October 2004 runs. The results of this study confirmed that coupled ocean-atmosphere models are clearly the next step towards improved climate forecasts along with better understanding of model biases on the monthly and seasonal timescales.

This study also led to insights on the physics used in the FSU/COAPS model. The hindcast runs are created by using updated weekly observed SSTs and the real-time runs use a less perfect method of persisted SSTA. Considering this, ideally the hindcast runs should consistently result in a more accurate forecast than the real-time runs. The fact that the hindcast runs occasionally produced poorer forecasts than the real-time runs leads to speculation that there are errors in the land-sea calculations used in the model; however, the real-time run's

performance over the hindcast run's could have been random since only two years were examined. Also, breaking down the seasonal temperature forecasts (DJF) into monthly forecasts revealed inconsistencies in the model's performance, with the exception of the constant under prediction (strong cold bias) of January (3 month lead time) temperatures. In addition to scattered predictability in the monthly temperature forecasts, the precipitation forecasts fell apart when examined on a monthly time scale, suggesting more errors in the model physics and indicating the model's monthly outlooks are not as confident as the seasonal forecasts.

Despite the findings with this study, these conclusions should be taken with caution. First of all, only two years of real-time runs were evaluated. In order to make statistically significant and confident conclusions about the real-time run's ability to forecast surface temperature and precipitation over the southeastern United States, more years of real-time model runs need to be examined. Also, because there were only three years of real-time runs available for this study, no long-term model climatology could be created specifically for the real-time runs. Instead, the hindcast climatology was used for both the real-time and hindcast runs bias correction and anomaly forecasts. This could have possibly led to a false sense of greater skill in the hindcast run compared to the real-time runs.

Although this study only evaluated two years of real-time runs, it serves as a springboard to future work. Obviously, more years of real-time runs can be examined to draw additional conclusions about the use of the FSU/COAPS climate model real-time runs for use in crop models. Evaluating more years of real-time runs to hindcast runs will offer valuable insight to the disadvantages of using prescribed SSTA in climate models and also connections between tropical SSTA and climate in the southeast. In addition, in-depth studies of possible errors in the model's physics should be examined using additional years of real-time and hindcast runs. Some other interesting studies that could stem from these results and would benefit both the agricultural and science community include: evaluating the model's ability to forecast in other seasons, examining in greater detail the model's skill in forecasting anomalous events (drought, heat waves, freeze events, flooding), comparing real-time and hindcast runs during strong ENSO events, and exploring the links between southeast climate (both temperature and precipitation) and tropical SSTA (in the Pacific as well as the Atlantic) in greater detail. Climate prediction is still far from perfect, but the FSU/COAPS climate model's ability to predict seasonal

temperature and precipitation patterns across the southeast suggest that the agricultural community could currently benefit from these climate forecasts.

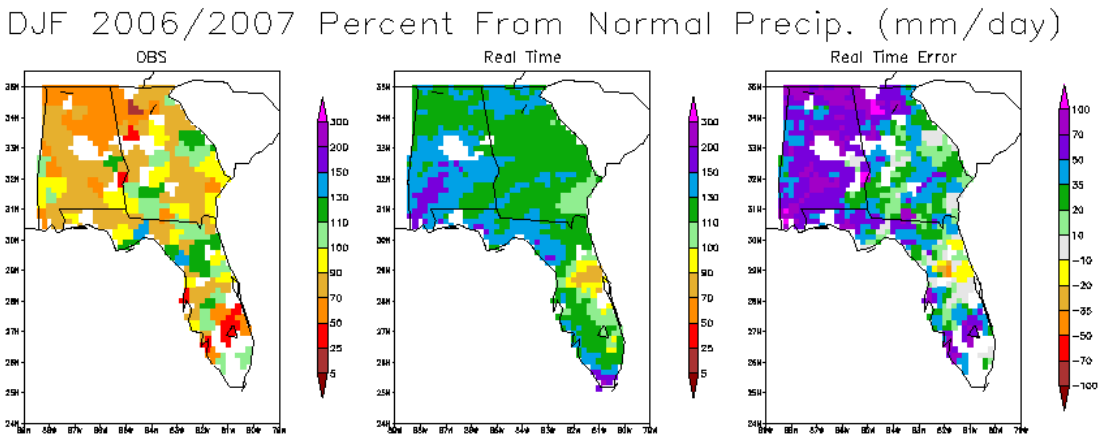

Figure 5.1. Spatial plots of the DJF 2006/2007 observed (left) and real-time (center) percent from normal precipitation. The error in the percent from normal precipitation from the October 2006 real-time runs (2 month lead time) is also plotted (right).

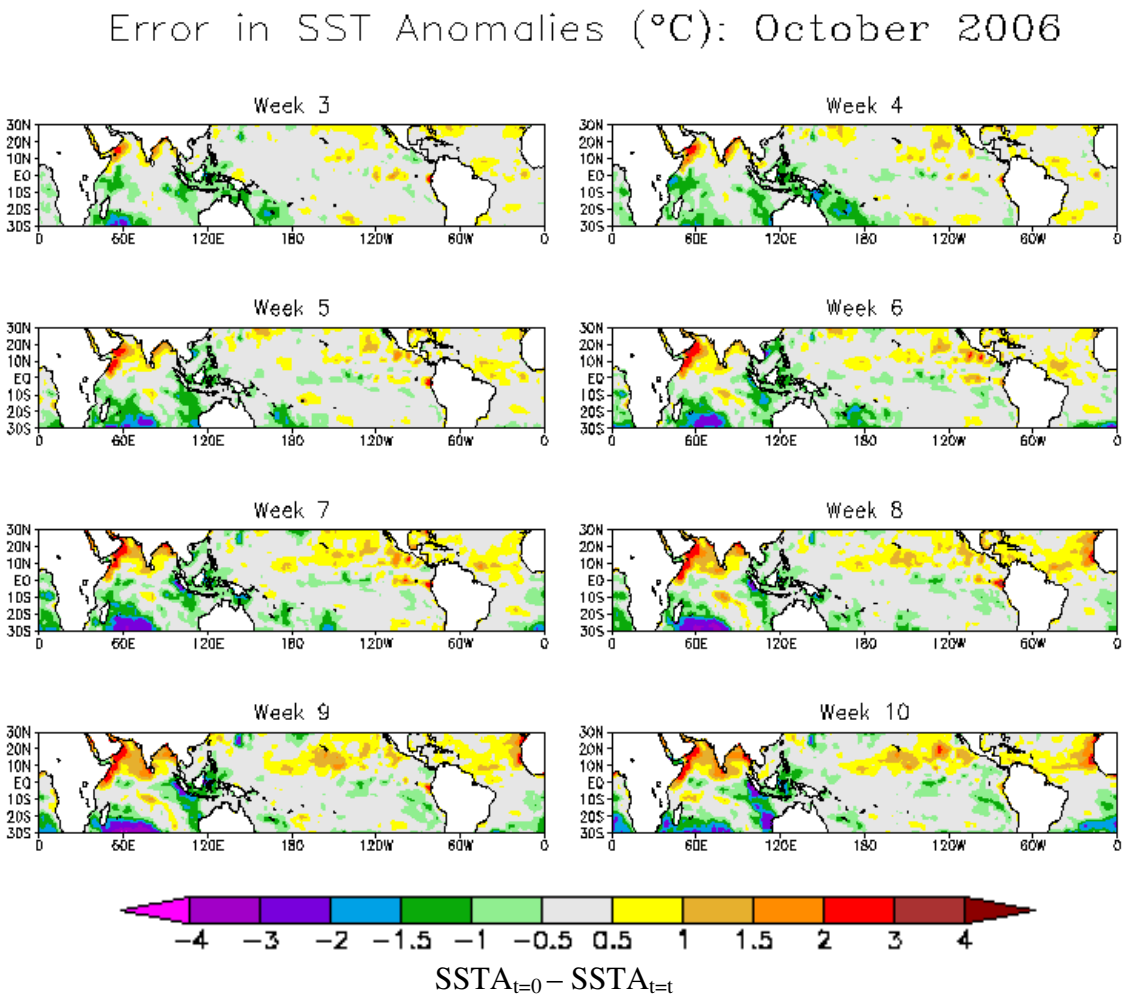

Figure 5.2. SSTA error growth (forecasted SSTA minus the observed SSTA) in the tropical Pacific (from weeks 3 through 10 of the forecast period) resulting from using a prescribed SSTA in the October 2006 real-time runs. The SST data originates from the National Center for Environmental Prediction Studies (NCEP's) Optimum Interpolation version two (OI.v2) dataset. The dataset is a combination of in situ SSTs, satellite SSTs, and SSTs simulated by sea-ice cover. More details of the reanalysis, including Reynold's method of bias correction for the satellite data is available at (www.emc.ncep.noaa.gov/research/cmb/sst_analysis/).

APPENDIX A
TAYLOR DIAGRAMS

The following formulas were used to create Taylor diagrams (Taylor, 2001):

Correlation:

$$\mathrm{R} = \frac{\frac{1}{\mathrm{N}} \sum_{n=1}^{N} \left(f_n - \bar{f}\right)\left(o_n - \bar{o}\right)}{\sigma_\mathrm{f}\, \sigma_\mathrm{o}}$$

Centered Root Mean Square (RMS) Difference:

$$\mathrm{E'}^2 = \frac{1}{\mathrm{N}} \sum_{n=1}^{N} \left[\left(f_n - \bar{f}\right) - \left(o_n - \bar{o}\right)\right]^2$$

Standard Deviation of Forecast:

$$\sigma_f{}^2 = \frac{1}{\mathrm{N}} \sum_{n=1}^{\mathrm{N}} \left(f_n - \bar{f}\right)^2$$

Standard Deviation of Observations:

$$\sigma_o{}^2 = \frac{1}{\mathrm{N}} \sum_{n=1}^{\mathrm{N}} \left(o_n - \bar{o}\right)^2$$

where N is the number of model grid points over the southeast, f_n is the forecasted variable at grid point n, $\bar{f}$ is the area average of the forecasted variable at each grid point, o_n is the observed variable at grid point n, and $\bar{o}$ is the area average of the observed variable at each grid point.

APPENDIX B

SKILL METRICS

1. Root Mean Squared Error (RMSE):

$$\mathrm{RMSE} = \sqrt{\frac{1}{\mathrm{N}} \sum_{n=1}^{N} (f_n - o_n)^2}$$

where N is the number of model grid points over the southeast, f_n is the forecasted variable at grid point n, and o_n is the observed variable at grid point n.

2. Brier Score (BS):

$$\mathrm{BS} = \frac{1}{\mathrm{N}} \sum_{n=1}^{N} (p_n - o_n)^2$$

where N is the number of model grid points over the southeast, p_n is the forecasted probability (determined from using five ensemble members) that an event at grid point n will occur, and o_n is what was observed (will equal 1 if the event occurred and 0 if the event did not occur).

$$\mathrm{BS}_{\mathrm{REF}} = \frac{1}{\mathrm{N}} \sum_{n=1}^{N} (\overline{o}_n - o_n)^2$$

where N is the number of model grid points over the southeast, $\overline{o}_n$ is the forecasted probability (determined from nineteen years of observed anomalies) that an event at grid point n will occur, and o_n is what was observed (will equal 1 if the event occurred and 0 if the event did not occur).

3. Relative Operating Characteristics (ROC) Curves: A plot of probability of detection (hit rate) vs. probability of false detection (false alarm rate). These rates are calculated for increasing (0.00, 0.20, 0.40, 0.60, 0.80, and 1.00) forecasted probability thresholds. The probabilities are determined from the five ensemble members. Hit rates and false alarm rates are calculated from the results of a contingency table:

Contingency Table				
	Observed			
Forecast		yes	No	Total
	yes	***hits***	***false alarms***	*forecast yes*
	no	***misses***	***correct negatives***	*forecast no*
	Total	*observed yes*	*Observed no*	*total*

POD (hit rate) = (hits) / (hits + misses)

POFD (false alarm rate) = (false alarms) / [(correct negatives + false alarms)]

3. Equitable Threat Scores (ETS): ETS is also determined from the results of a contingency table, similar to the one seen with the ROC curves explanation.

$$ETS = (hits - hits_{random})/(hits + misses + false\ alarms - hits_{random})$$

$$Hits_{random} = [(hits + misses)(hits + false\ alarms)] / total$$

REFERENCES

Bjerknes, J., 1966: A possible response of the atmospheric Hadley circulation to equatorial anomalies of ocean temperature. *Tellus*, **18**, 820-829.

——, 1969: Atmospheric teleconnections from the equatorial Pacific. *Mon. Wea. Rev.*, **97**, 163-172.

Cocke, S., and T. E. LaRow, 2000: Seasonal predictions using a regional spectral model embedded within a coupled ocean-atmosphere model. *Mon. Wea. Rev.*, **128**, 689–708.

——, ——, and D. W. Shin,2007: Seasonal rainfall predictions over the southeast United States using the Florida State University nested regional spectral model, *J. Geophys. Res.*, 112, D04106, doi:10.1029/2006JD007535.

Gershunov, A., and T. P. Barnett, 1998: ENSO influence on intraseasonal extreme rainfall and temperature frequencies in the contiguous United States: Observations and model results. *J. Climate,* **11,** 1575–1586.

Goddard, L., and S. J. Mason, 2002: Sensitivity of seasonal climate forecasts to persisted SST anomalies. *ClimateDyn.,* **19**, 619–631, doi:10.1007/s00382-002-0251-y.

——, ——, S. E. Zebiak, C. F. Ropelewski, R. Basher and M. A. Cane, 2001: Current approaches to seasonal-to-interannual climate predictions. *Int. J. Climatol.*, **21**, 1111-1152.

Hansen, J. W., A. W. Hodges, and J. W. Jones, 1998: ENSO influences on agriculture in the southeastern United States, *J. Climate,* **11,** 404–411.

Hogan, T. F., and T. E. Rosmond, 1991: The description of the U.S. Navy Operational Global Atmospheric Prediction System's spectral forecast model. *Mon. Wea. Rev.,* **119**, 1786–1815.

Hurlburt, H. J., J. Kindle, and J. J. O'Brien, 1976: A numerical simulation of the onset of El Niño. *J. Phys. Oceanogr.,* **6**, 621–631

Lim, Young-Kwon, D. W. Shin, Steven Cocke, T. E. LaRow, Justin T. Schoof, James J. O'Brien, and Eric P. Chassignet, 2007: Dynamically and statistically downscaled seasonal simulations of maximum surface air temperature over the southeastern United States, *J Geophys Res*, *112*, D24102, doi:10.1029/2007JD008764.

Montroy, D., 1997: Linear relation of central and eastern North American precipitation to tropical Pacific sea surface temperature anomalies. *J. Climate,* **10,** 541–558.

Palmer, T. N., F. Molteni, R. Mureau, R. Buizza, P. Chapelet, and J. Tribbia, 1993: Ensemble prediction. *Proc. Validation of Models over Europe,* Vol. 1, Shinfield Park, Reading, United Kingdom, ECMWF, 21–66.

Reynolds, R. W., N. A. Rayner, T. M. Smith, D. C. Stokes, and W. Wang, 2002: An improved in situ and satellite SST analysis. *J. Climate,* **15,** 1609–1625.

Ropelewski, C. F., and M. S. Halpert, 1986: North American precipitation and temperature patterns associated with the El Niño/Southern Oscillation (ENSO). *Mon. Wea. Rev.,* **114,** 2352–2362.

——, and ——, 1987: Global and regional scale precipitation patterns associated with the El Niño/Southern Oscillation. *Mon. Wea. Rev.,* **115,** 1606–1626.

——, and ——, 1989: Precipitation patterns associated with the high index phase of the Southern Oscillation. *J. Climate,* **2,** 268–284.

Shin, D.W., S. Cocke, T.E. LaRow, and J.J. O'Brien. 2005. Seasonal surface air temperature and precipitation in the FSU Climate Model coupled to the CLM2. J. Climate, 18: 3217-3228.

Smith, S. R., D. M. Legler, M. J. Remigio, and J. J. O'Brien, 1999:Comparison of 1997-98 U.S. temperature and precipitation anomalies to historical ENSO warm phases. *J. Climate,* **12,** 3507–3515.

Taylor, K.E., 2001: Summarizing multiple aspects of model performance in a single diagram. *J. Geophys. Res.,* **106**, 7183-7192.

Tracton, M. S., and E. Kalnay, 1993: Operational ensemble prediction at the National Meteorological Center: Practical aspects. *Wea. Forecasting,* **8,** 379–398.

Wilks D. S., 1995: *Statistical Methods in the Atmospheric Sciences*. Academic Press, 467 pp.

——, and R. L. Wilby, 1999: The weather generation game: A review of stochastic weather models. *Prog. Phys. Geogr.*, **23**, 329–357.

Wyrtki, K., 1975: El Nino – the dynamic response of the equatorial Pacific Ocean to atmospheric forcing. *J. Phys. Ocean.*, **5**, 572-584.

BIOGRAPHICAL SKETCH

Mary Beth was born and raised in Exton, Pa, a Philadelphia suburb. She developed a passion for meteorology at the early age of five and would frequently be found watching The Weather Channel, standing outside during thunderstorms, or praying for major snow storms. Being from Pennsylvania, it only seemed natural to attend the Pennsylvania State University. She proudly graduated from Penn State in 2006 and obtained a Bachelor of Science degree in Meteorology with a forecasting and communications option, but was not completely satisfied. Still eager to learn more about the atmosphere, she signed up to attend graduate school for meteorology at Florida State University in the Fall of 2006. In January 2008, she accepted a job with NOAA's (National Oceanic and Atmospheric Administration) National Weather Service.

Mary Beth currently resides in the Washington, DC suburbs and enjoys working as a surface analyst for the HPC (Hydrometeorological Prediction Center), one of NCEP's (National Center for Environmental Prediction) national centers. After she completes her master's degree from Florida State, she is really looking forward to focusing on her career within the National Weather Service and spending more quality time with her family and future husband, also a meteorologist.